Published in : ACS Macro Letters (2021), vol. 10, n°03, pp. 313-320
DOI: 10.1021/acsmacrolett.1c000337
Status : Postprint (Author's version)

FUNCTIONAL POLYETHYLENES BY ORGANOMETALLIC-MEDIATED RADICAL POLYMERIZATION OF BIOBASED CARBONATES

Philip B. V. Scholten, Grégory Cartigny, Bruno Grignard, Antoine Debuigne, Henri Cramail, Michael A. R. Meier, and Christophe Detrembleur

Philip B. V. Scholten, Center for Education and Research on Macromolecules (CERM), CESAM Research Unit, Department of Chemistry, University of Liège, 4000 Liège, Belgium; Institute of Organic Chemistry, Materialwissenschaftliches Zentrum MZE, Karlsruhe Institute of Technology, 76131 Karlsruhe, Germany;

Grégory Cartigny, Bruno Grignard, Antoine Debuigne, Cristophe Detrembleur, Center for Education and Research on Macromolecules (CERM), CESAM Research Unit, Department of Chemistry, University of Liège, 4000 Liège, Belgium;

Henri Cramail, Laboratoire de Chimie des Polymères Organiques (LCPO), Université de Bordeaux, 33607 Pessac, France ;

Michael A.R. Meier, Institute of Organic Chemistry, Materialwissenschaftliches Zentrum MZE, Karlsruhe Institute of Technology, 76131 Karlsruhe, Germany; Laboratory of Applied Chemistry, Institute of Toxicology and Genetics (ITG), Karlsruhe Institute of Technology (KIT), 76344 Eggenstein-Leopoldshafen, Germany

Keywords :

Copolymerization, Copolymers, Hydrocarbons, Inorganic Carbon Compounds, Monomers

Abstract

Partly or fully renewable (co)polymers are gaining interest in both academia and industry. Polyethylene is a widely used polymer, classically derived from fossil fuels, with a high versatility stemming from the introduction of comonomers altering the mechanical properties. The introduction of renewable functionalities into this polymer is highly attractive to obtain functional, tunable, and at least partially renewable polyethylenes. We herein report the introduction of biosourced cyclic carbonates into polyethylene using organometallic-mediated radical polymerization under mild conditions. Molecular weights of up to 14 600 g mol^{-1} with dispersities as low as 1.19 were obtained, and the cyclic carbonate content could be easily tuned by the ethylene pressure during the polymerization. As a proof of concept, the hydrolysis of the cyclic carbonates of a representative copolymer was explored, and it provided polyethylene-bearing vicinal diols, with a hydrolysis degree of 71%. Given the multitude of chemoselective modifications possible on cyclic carbonates as well as the fact that many allylic- and alkylidene-type cyclic carbonates are accessible from renewable resources, this work opens up an avenue for the design of functional and more sustainable polyethylenes.

Polyethylene (PE) is a ubiquitous material in our daily life, least partially renewable PEs. Among other techniques, these constituting ∼30% of the European polymer market,[1,2] cyclic carbonates have been polymerized by free-radical and is primarily produced by free-radical or coordination−insertion polymerizations.[3] Biosourced ethylene derived from, for example, sugar cane, has allowed the synthesis of fully biobased PE on an industrial scale.[4] One key advantage of PE is that its properties can be easily tuned for a particular application by introducing polar moieties. Currently, these polar functional groups are mainly limited to carboxylic acids, ketones and esters, and it remains challenging to control their incorporation over a broad composition range[5–7] and thus access the whole property spectrum of functional PE. Moreover, the polar comonomers used are rarely renewably sourced, obtained in a sustainable fashion, or incorporated into polymers with defined molecular weights. Overcoming the combined challenge of synthesizing molecularly defined Pes with novel polar comonomers obtained from renewable resources in a sustainable fashion with the ability to easily tune the comonomer content has thus far not been possible and would constitute a significant step toward functional and renewable PEs.

Cyclic carbonates are very versatile examples of renewable and functional molecules that have recently gained importance within polymer science,[8,9] as they offer a variety of (chemo)-selective transformations[10–16] and can be synthesized from renewable resources, such as CO2[17–23] and plant oils.[24,25] The combination of vinyl monomers bearing cyclic carbonates with ethylene thus offers the possibility to obtain functional and at least partially renewable PEs. Among other techniques, these cyclic carbonates have been polymerized by free-radical polymerizations (FRPs)[26–29] and recently also by reversible deactivation radical polymerization (RDRP).[12,30–32] The latter used cyclic carbonate monomers bearing an acrylate, α-alkylidene, or allylic double bond, which, to date, are not polymerizable with ethylene using RDRP, mainly because of the monomer reactivity difference.[6,7] In particular, terminal allylic groups are extremely challenging to polymerize, in general, as a result of the degradative chain transfer from the growing radical chain to the allyl-type monomer, forming a stabilized allyl radical with a low propagation rate, which halts the polymerization.[33–37] Nonetheless, the aforementioned α-alkylidene and allylic cyclic carbonate monomers (**Scheme 1**) are highly interesting for functional ethylene-based copolymers.

Such renewable cyclic carbonates appear even more attractive in light of recent breakthroughs in the RDRP of ethylene, allowing tuning of the comonomer incorporation over a large range, from 5 to 80 mol % for some comonomers, while at the same time controlling the copolymer's molecular parameters.[38–43] This was possible for a selected number of less-activated polar monomers bearing an unconjugated double bond such as vinyl esters,[38,39,44] vinyl ethers,[40] N-vinyl amides,[38,40] or cyclic ketene acetals,[42] which are mostly obtained from nonrenewable resources. In addition, post-polymerization modifications for these polymers, aside from hydrolysis, are difficult.

In the quest for new PE functionalities obtained from renewable monomers, we considered the RDRP of ethylene (**E**) with allyl ((2-oxo-1,3-dioxolan-4-yl)methyl) carbonate (**M1**, **Scheme 1**) and 4,4-dimethyl-5-methylene-1,3-dioxolan-2-one (**M2**, **Scheme 1**). **M1** is produced in a sustainable fashion from renewable glycerol and dimethyl carbonate (DMC) through transesterifications,[32] whereas **M2** is partially renewable and is obtained from the quantitative organocatalyzed coupling of CO_2 and 2-methyl-3-butyn-2-ol alcohol.[45] The copolymerizations were investigated using an organocobalt complex, R-Co(acac)$_2$, as the initiator and controlling agent (**Scheme 1**). This organometallic-mediated radical polymerization (OMRP) process was selected because it is highly performing for less activated monomers, such as vinyl esters and ethylene, under mild conditions (i.e., 40 °C).[46] These were expected to disfavor side reactions that are commonly encountered during the polymerization of ethylene[47] and allylic-[48,49] and α-alkylidene-type[27] monomers. Under these OMRP conditions, the allylic- (**M1**) and α-alkylidene-bearing (**M2**) cyclic carbonate monomers could previously not be homopolymerized but were statistically copolymerized with vinyl acetate.[12,32] On the contrary, the OMRP of ethylene was possible only at high pressures (500 bar) and relatively high temperatures (60−80 °C) and furnished low-molar-mass PE with only poor control over the molecular structure.[38,50] The copolymerizations reported herein were performed in autoclaves (**Figure S1**) at ethylene pressures ranging from 10 to 500 bar in DMC (**Scheme 1**), a solvent with a low transfer to solvent constant in ethylene polymerizations.[51]

Scheme 1. Synthetic Pathways to Fully Renewable and Sustainable Cyclic Carbonate Monomer **M1** and Partially Renewable Cyclic Carbonate **M2** as Well as Renewable Ethylene[a]

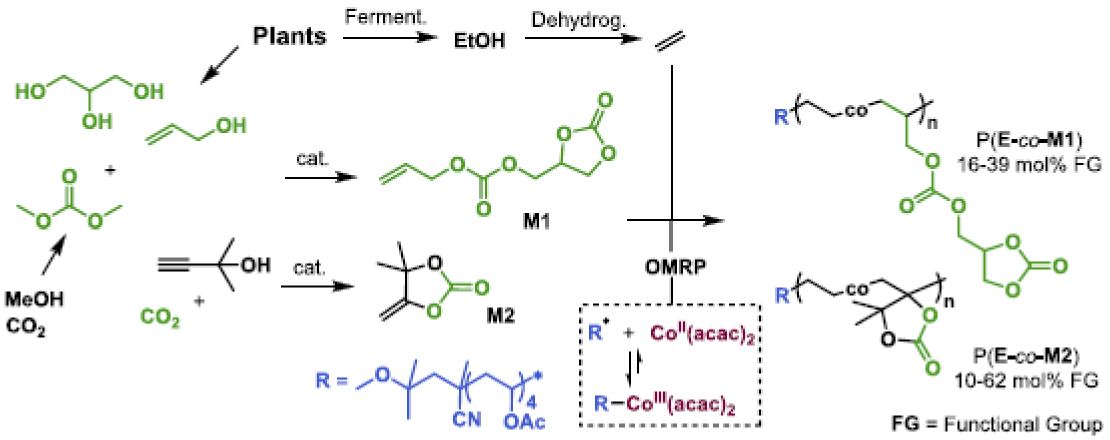

[a]Organometallic-mediated radical copolymerization of these monomers leads to functional and renewable polyethylene with a tunable amount of cyclic carbonate content.

First, we initiated the copolymerizations of **M1** or **M2** with ethylene (**E**) by R-Co(acac)$_2$ at 40 °C and 50 bar of ethylene pressure, which was kept constant during the whole polymerization process. The polymerization kinetics were followed through separate experiments carried out for 2, 4, 8, and 24 h, as the withdrawal of samples during the pressurized polymerization was not possible. All copolymers were soluble in tetrahydrofuran (THF) and were thus analyzed by size-exclusion chromatography (SEC) in THF. For both monomers, a linear increase in the number-average molar mass (M_n) with conversion was observed (**Figure 1a**,**b**), which is in line with a controlled chain growth. In addition, the dispersities were low for both the **E**/**M1** and **E**/**M2** copolymerizations ($1.10 \leq Đ \leq 1.40$; **Figure 1a**,**b**). This dispersity, however, increased to 1.88 for the **E**/**M1** copolymerization after 24 h. Importantly, the comonomer content of ∼20 mol % was measured for both **M1** and **M2** throughout the 24 h of polymerization, emphasizing the constant incorporation of the comonomers in the PE chains at this working pressure. **Figure 1c**, **d** shows that the SEC chromatograms were shifted toward the higher molar mass side during polymerization. Note that the crude samples were analyzed to avoid any fractionation of the polymer during purification, resulting in a small peak at 20 min of elution that corresponded to some deactivated RCo(acac)$_2$. This was removed once the polymer was purified using supercritical CO$_2$ (scCO$_2$) extraction (see the **Supporting Information**), which also enabled the facile recycling of the remaining monomer.[32] Alternatively, dialysis could also be used as a less sustainable means of purification (see the Supporting Information). Although the conversion of the renewable comonomers may seem low (<14%), it is important to highlight that analogous coordination−insertion polymerizations with polar monomers, in particular, allylic ones, are typically limited to <10% conversion.[52−59] The increase in the M_n with the polymer yield, the rather low dispersities, and the monomodal molar mass distributions were also confirmed for the P(**E**-*co*-**M2**) kinetic study using high-temperature SEC analyses in trichlorobenzene (TCB) at 140 °C (**Figure S3**), as this polymer was soluble in TCB, unlike P(**E**-*co*-**M1**). The insolubility of the P(**E**-*co*-**M1**) copolymer in TCB was assumed to be the result of the higher polarity of the copolymer, with the presence of two carbonate groups per comonomer unit.

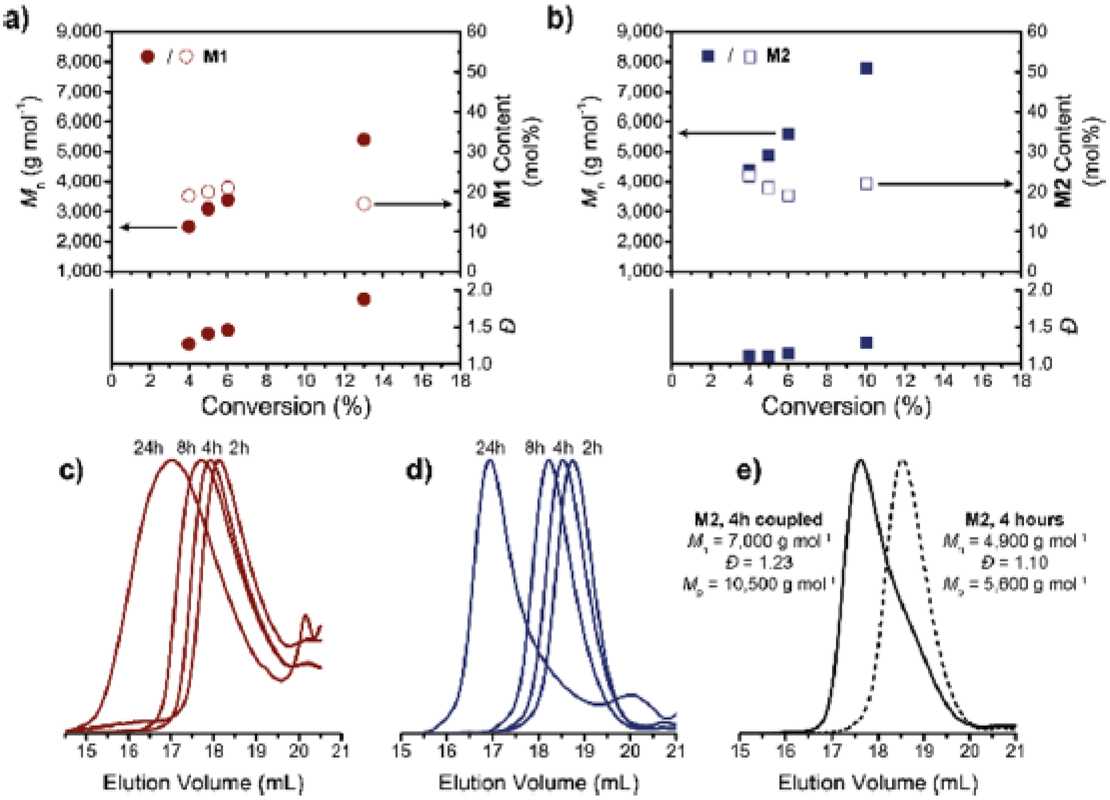

Figure 1. Plot of polymer number-average molar mass (M_n), dispersity (*Đ*), and comonomer content in the copolymer versus conversion for the OMRP of ethylene with (a) 2.5 mmol of **M1** in 2.5 mL of DMC and (b) 10 mmol **M2** in 5 mL of DMC. (c) Corresponding SEC curves and (e) SEC traces of an **E**/**M2** polymerization before (dashed line) and after (solid line) the addition of isoprene. Copolymerization conditions: [**M1** or **M2**]/ [R-Co] = 100, 50 bar **E**, 40 °C, 500 rpm, reactor volume = 30 mL; coupling conditions: 17.5 mmol isoprene, 40 °C.

To probe the chain-end fidelity of the polymer chains during the polymerization, isoprene-assisted radical coupling was performed.[60,61] It consists of the addition of isoprene to the polymerization medium after 4 h of reaction (see the **Supporting Information** for details) and should result in the immediate quantitative coupling of polymer chains end-capped by the cobalt complex. This technique has been widely exploited to prepare symmetrical triblock copolymers by coupling diblock copolymers end-capped by $Co(acac)_2$ or to probe the living character of chains prepared by OMRP.[38,60−63] For **M1**, SEC chromatograms (in THF) remained unchanged after the addition of isoprene (**Figure S4**), suggesting the absence of chain coupling. Several attempts were carried out with the same observation. Because the kinetic investigations for the **E**/**M1** copolymerization without isoprene evidenced a linear chain growth during the polymerization after 4 h of reaction (**Figure 1a**), we hypothesized that the polymer chains were not able to react with isoprene, most likely because of their deactivation or lack of solubility in the reactor after depressurization prior to the injection of isoprene. A lack of solubility leading to the precipitation and deactivation or side reactions of the growing polymer chains in the polymerization medium has been previously reported.[50,64] On the contrary, the P(**E**-*co*-**M2**) chains were successfully coupled under similar conditions, as illustrated by the SEC chromatogram shift (in THF) of the copolymer from a peak average molar mass (M_p) of 5600−10 500 g mol^{-1} after the reaction (**Figure 1e**), although a small tailing was observed in the SEC chromatogram. This experiment demonstrated that most of the P(**E**-*co*-**M2**) chains were still end-capped by $Co(acac)_2$ when isoprene was added.

Table 1. Copolymerization of **E** with **M1** in Dimethyl Carbonate (DMC)[a]

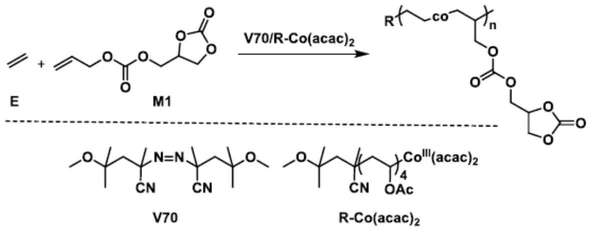

entry	P (bar)[b]	yield (mg)	X_M (mol %)[c]	M_n (g mol^{-1})[d]	$Đ$[d]	T_g (°C)[e]	T_m (°C)[e]	cryst (%)[e]
1[f]	50	56	28	7000	1.58	n.d.	n.d.	n.d.
2	10	<10	n.d.	1400	1.69	n.d.	n.d.	n.d.
3	25	32	39	2000	1.87	−52		
4	50	72	17	5500	1.59	5	46	4.5
5	500	86	16	ins.	ins.	3	108	9.6

[a] Polymerization conditions: 40 °C, 24 h, 500 rpm, DMC = 2.5 mL, **M1**/R-$Co(acac)_2$ = 100, **M1** = 2.5 mmol. [b] Ethylene pressure (bar). [c] X_M = comonomer incorporation (mol %), determined by ^1H NMR spectroscopy in a 2:1 v/v mixture of TCE/C_6D_6 on a 400 MHz spectrometer at 80 °C using the α-chain end (see the **Supporting Information**). [d] Determined by SEC in tetrahydrofuran (THF) at 40 °C using a polystyrene standard. [e] T_g, glass-transition temperature (°C); cryst, copolymer crystallinity (%); determined by differential scanning calorimetry (DSC). Cryst = (ΔH_m measured/$\Delta H_{m\infty}$) × 100, where $\Delta H_{m\infty}$ = 293 J g^{-1}. [f] Use of V70 instead of R-$Co(acac)_2$; V70 = 0.012 mmol, **M1**/R-$Co(acac)_2$ = 100. n.d., not determined; ins., insoluble in THF.

Table 2. Copolymerizations of **E** with **M2** in Dymethyl Carbonate (DMC)[a]

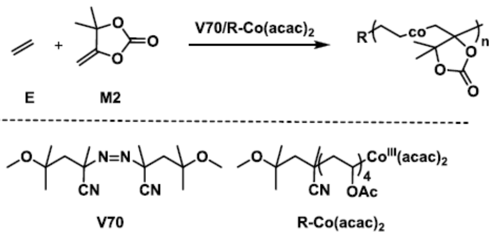

entry	*P* (bar)[b]	yield (mg)	X_M (mol %)[c]	M_n (g mol^{-1})[d]	Đ[d]	T_g (°C)[e]	T_m (°C)[e]	cryst (%)[e]
1[f]	50	67	20	9600	1.61	n.d.	n.d.	n.d.
2	10	67	62	2200	1.21	27		
3	25	163	34	3400	1.22	17		
4	50	224	22	8100	1.28	2	49	5
5	500	162	10	ins.	ins.	n.o.	90	15

[a]Polymerization conditions: 40 °C, 24 h, 500 rpm, DMC = 5 mL, **M2**/R-Co(acac)$_2$ = 100, M2 = 10 mmol. [b]Ethylene pressure (bar). [c]X_M, comonomer incorporation (mol %), determined by elemental analysis. [d]Determined using SEC in tetrahydrofuran (THF) at 40 °C using a polystyrene standard. [e]T_g, glass-transition temperature (°C); cryst, copolymer crystallinity (%); determined by differential scanning calorimetry (DSC). Cryst = (ΔH_m measured/$\Delta H_{m\infty}$) × 100, where $\Delta H_{m\infty}$ = 293 J g^{-1}. [f]Use of V70 instead of R-Co(acac)$_2$; V70 = 0.05 mmol, **M2**/RCo(acac)$_2$ = 100. n.d., not determined; Ins., insoluble in THF; n.o., not observable.

In comparison with the above OMRPs, FRP using a conventional initiator under otherwise identical conditions led to lower polymer yields for the **E**/**M1** (comparison of entries 1 and 4, **Table 1**) and to lower polymer yields and higher dispersities for the **E**/**M2** copolymerizations (comparison of entries 1 and 4, **Table 2**). Because the propagating rate constant of the monomers is mainly governed by the reaction conditions, that is, the solvent, concentration, and temperature, the difference in yields between FRP and OMRP was mainly attributed to the decrease in irreversible side reactions that deactivate the growing chains.

Figure 2 depicts the ^{1}H and ^{13}C NMR spectra of P(**E**-co-**M1**) synthesized at 50 bar in DMC at 40 °C and quenched with TEMPO after 24 h (entry 4, **Table 1**). The broad signals at 3.96 (n, q, s) and 4.40 ppm (r) correspond to the −CH$_2$− and −CH− groups of the comonomer **M1** neighbor to the carbonate functionalities (**Figure 2a**). Signals characteristic of the initiator *α*-chain end were observed at 0.80 (c, f), 1.65 (h), 1.86 (k), 2.98 (a), and 4.84 ppm (i), whereas the intense peak at 1.18 ppm (u) originated from the −CH$_2$− of the ethylene repeat units. Using the methoxy α-chain end peak, the molecular weight of the P(**E**-co-**M1**) copolymer was calculated to be 4000 g mol^{-1} from the ^{1}H NMR spectrum. In the ^{13}C NMR spectrum (**Figure 2b**), the signals at 38 (m), 66 (q, s), 72 (n), and 155 ppm (t, o) confirm the successful incorporation of **M1** into the copolymer. Furthermore, resonances at 27 (z) and 32 ppm (l) highlight the ethylene-carbonate motif present in the polymer backbone. These assignments were supported by COSY and HSQC NMR analyses (**Figures S5** and **S6**). Further NMR and FT-IR spectra as well as the fully assigned spectra of P(**E**-co-**M2**) synthesized at 50 bar (entry 4, **Table 2**) can be found in the **Supporting Information** (**Figures S7−S11**) and are in line with the targeted copolymer structure. The molecular weight was also calculated by ^{1}H NMR spectroscopy for P(**E**-co-**M2**) based on the *α*-chain end and was found to be 4900 g mol^{-1} (**Figure S9a**).

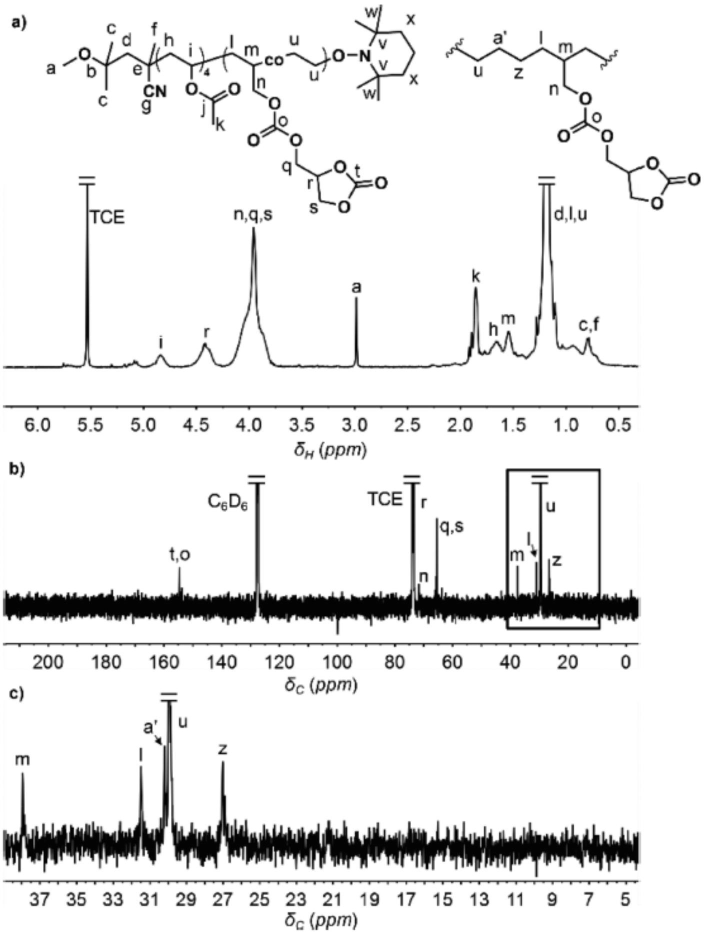

Figure 2. (a) ^{1}H and (b) ^{13}C NMR spectra and (c) inset of the ^{13}C NMR spectrum in the 4−38 ppm region for P(**E**-co-**M1**) (entry 4, **Table 1**) taken in a 2:1 v/v mixture of tetrachloroethane (TCE)/ benzene (C_6D_6) on a 400 MHz spectrometer at 80 °C.

The influence of the ethylene pressure on the carbonate content for copolymers P(**E**-co-**M1**) and P(**E**-co-**M2**) was then evaluated. Pressures ranging from 10 to 500 bar were tested, and all reactions were stopped after 24 h (entries 2−5, **Tables 1** and **2**). The composition of the resulting copolymers was determined by ^{1}H NMR spectroscopy for **M1**-based copolymers and by elemental analysis for **M2**-containing copolymers. ^{1}H NMR analyses were performed in a deuterated solvent mixture of 1,1,2,2-tetrachloroethane and benzene (TCE/C_6D_6) at 80 °C, which enabled the solubilization of all copolymers. Indeed, $CDCl_3$ was not able to solubilize the copolymers prepared at 500 bar. The composition of P(**E**-co-**M2**) could, however, not be determined by ^{1}H NMR in TCE/C_6D_6 because the characteristic resonances of this monomer overlapped with those of ethylene (see **Figure S9** in the **Supporting Information**), justifying the use of elemental analysis. Copolymerizations of **E**/**M1** at lower pressures (10 and 25 bar) led to very low yields (<10 and 32 mg; entries 2 and 3, **Table 1**), and the analysis of P(**E**-co-**M1**) prepared at 10 bar was not possible. At 25 bar, an incorporation of 39 mol % of comonomer was noted. By increasing the ethylene pressure to 50 bar, the yield was more than doubled, and the comonomer content was decreased to 17 mol % (entry 4, **Table 1**) as more ethylene was involved in the process. A further increase in the working pressure to 500 bar improved the yield while preserving 16 mol % of comonomer within the copolymer (entry 5, **Table 1**). It appeared that at this pressure (500 bar) the maximum content of ethylene in the copolymer was reached (84 mol %).

For the **E**/**M2** copolymerization, the same trend was noted with an increased yield and decreased comonomer content in the copolymer with an increased working pressure (from 62 mol % at 10 bar to 10 mol % at 500 bar; entries 2 and 5, **Table 2**). It must be noted that the yield was surprisingly low at 500 bar compared with the experiment performed at 50 bar. This result was reproducible, suggesting a slowing down of the polymerization at this high ethylene pressure and thus when more ethylene was incorporated into the growing chain. To give a better appreciation of the obtained yields, the theoretical maximum yield was calculated (see **Table S1**, **Supporting Information**) and was found to be <10% for all polymerizations.

The decrease in carbonate content in the copolymers as a function of the ethylene working pressure can be neatly followed via FT-IR spectroscopy by comparing the relative intensities of the stretching vibrations of the cyclic carbonate of the **M2** repeating unit (1800 cm^{-1}, highlighted in green) and $-CH_2-$ of the ethylene monomer unit (2800 cm^{-1} highlighted in gray; **Figure S11**). All of these results illustrate that PEs bearing cyclic carbonate pendants are now accessible over a broad composition range, from 62 to 10 mol % of functional comonomer **M2**, by adjusting the working pressure from 10 to 500 bar. Note that the composition calculated for P(**E**-co-**M2**) by elemental analysis was confirmed by ^1H NMR analysis in $CDCl_3$ of a copolymer that was fully soluble in this solvent (**Table 2**, entry 4). In this solvent, the peak separation was strongly improved (**Figure S9**), yielding a composition that was very similar to the one obtained by elemental analysis (EA) (17 mol % by EA and 18 mol % by NMR).

For both copolymerizations, the M_n and yield increased with the pressure. For P(**E**-co-**M1**), the M_n increased from 1400 g mol^{-1} at 10 bar to 5500 g mol^{-1} at 50 bar. For P(**E**-co-**M2**), the M_n increased from 2200 to 8100 g mol^{-1} going from 10 to 50 bar of ethylene with a rather low dispersity ($Đ$ = 1.21 to 1.28; entries 2–4, **Table 2**) and monomodal distributions (**Figure S12**). It should be noted that the P(**E**-co-**M2**) copolymer synthesized at 500 bar showed a slight shoulder at the higher molar mass side that increased the M_n (**Figure S12**). At this stage, it is, however, not possible to determine whether this side reaction occurred during the polymerization or during the isolation of the polymer. A P(**E**-co-**M2**) of higher M_n (14 600 g mol^{-1}) with a low dispersity of 1.19 could also be prepared by increasing the [M2]/[R-Co] ratio to 300 at 50 bar (**Figure S13**). Note that the copolymers synthesized by OMRP with the highest ethylene content (entry 5, **Tables 1** and **2**) were insoluble in THF. To analyze these, SEC analyses in TCB at 140 °C were performed and are shown in **Figure S14** and **Tables S2** and **S3**. These results clearly show a further increase in M_n from 50 to 500 bar of ethylene pressure.

The thermal analysis of the copolymers by differential scanning calorimetry (DSC) showed clear glass-transition temperatures (T_g) for all copolymers synthesized below 500 bar (**Table 1**), suggesting a random incorporation of the polar monomer. For P(**E**-co-**M1**), the T_g was found to increase with an increasing ethylene content from −52 °C at 25 bar to 5 and 3 °C at 50 and 500 bar, respectively. The opposite was true for P(**E**-co-**M2**), for which a decrease in T_g from 27 °C at 10 bar to 2 °C at 50 bar was observed. Moreover, the copolymers synthesized at 50 and 500 bar presented a semicrystalline behavior as a result of their high ethylene content, >78 mol % (entries 4 and 5, **Tables 1** and **2**; **Figure S15**). The melting temperatures (T_m) of the copolymers with high polar monomer content were strongly reduced, down to 46 °C (entry 4, **Tables 1** and **2**), compared with regular PE (T_m = 110–130 °C)[3] and were observed to be broad, that is, over a large range of temperatures (**Figure S15**), which is analogous to previously reported ethylene copolymers containing polar comonomers.[55,58,65,66] As a result of this broad T_m, a clear identification of a T_g was not possible for P(**E**-co-**M2**) synthesized at 500 bar (Figure

S15b). It should be noted that the copolymers do not have the same M_n, which strongly impacts their crystallinity, as observed for P(**E**-co-**M1**) synthesized at 50 and 500 bar, which contained the same amount of polar monomer (16 mol %) but had different crystallinities (4.5 and 9.5%, respectively; entries 4 and 5, **Table 1**).

As previously mentioned, the cyclic carbonate units in these PEs can be further exploited for functionalizations. To exemplify this, a P(**E**-co-**M2**) copolymer was hydrolyzed in ethanol in the presence of KOH at 75 °C under reflux for 32 h (see **Scheme 2** and the **SI** for experimental details). After purification, ^{1}H NMR spectroscopy (**Figure S17**) evidenced that 71% of the cyclic carbonates were hydrolyzed, leading to the formation of an unprecedented PE copolymer bearing vicinal diols. The chemical structure was further supported by ^{13}C and COSY NMR spectroscopy (**Figures S17**−**S20**) and FT-IR spectroscopy (**Figures S20**).

In conclusion, we herein show that renewable and functional PE copolymers can be obtained by the OMRP of ethylene with a CO_2-based α-alkylidene carbonate or a fully renewable and **Scheme 2**. Reaction Scheme for the Hydrolysis of P(**E**-co-**M2**) sustainably obtained cyclic carbonate bearing an allylic double bond. The facile tuning of the comonomer content, by simply changing the working pressure, allows close control of the cyclic carbonate units installed along the backbone of such PE copolymers. In addition, the cyclic carbonates were exploited to form PE-bearing vicinal diols by hydrolysis of the cyclic carbonate groups. Because the cyclic carbonates are reactive toward various nucleophiles, a multitude of valuable pending functions (diols, linear carbonates, carbamates, etc.) can be introduced from these carbonates, providing new opportunities to closely adjust the properties of PE for a range of applications.

Scheme 2. Reaction Scheme for the Hydrolysis of P(E-co-M2)

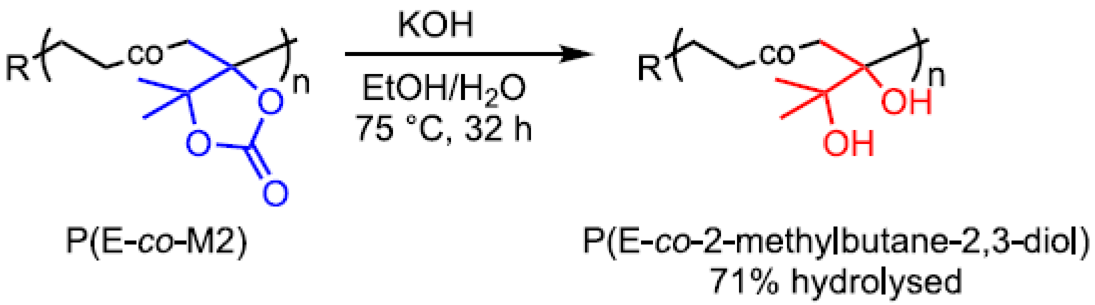

Published in : ACS Macro Letters (2021), vol. 10, n°03, pp. 313-320
DOI: 10.1021/acsmacrolett.1c000337
Status : Postprint (Author's version)

ASSOCIATED CONTENT

SUPPORTING INFORMATION

1. MATERIALS

Dimethylcarbonate (DMC; ≥99%, Merck) was degassed and dried over 4 Å molecular sieves. Alkyl cobalt(III) adduct ([Co(acac)$_2$(-CH(OCOCH$_3$)CH$_2$)$_{<4}$-R$_0$] with R$_0$ being the primary radical generated by V-70, from now on R-Co(acac)$_2$), was prepared according to a previous literature report and stored at -20 °C in CH$_2$Cl$_2$.[1] Ethylene (**E**; N35, 99.95%, AirLiquide), 2,2,6,6-tetramethyl-1-piperidinyloxy (TEMPO; 98%, Aldrich), tetrahydrofuran (THF, ≥99.9%, VWR), chloroform-*d* (CDCl3; >99%, euriso-top), 1,1,2,2-tetra-chloroethane-*d*$_2$ (TCE; ≥99%, euriso-top), benzene-*d*$_6$ (C6D6; ≥99%, euriso-top), 2,2'-azobis(4-methoxy-2,4-dimethylvaleronitrile) (V-70; Wako Pure Chemicals), 1,2,4-trichlorobenzene (TCB; >99%, Aldrich), and 3 and 4 Å molecular sieves (Sigma-Aldrich) were used as received. Allyl ((2-oxo-1,3-dioxolan-4-yl)methyl) carbonate (**M1**), and 4,4-dimethyl-5-methylene-1,3-dioxolan-2-one (**M2**) were prepared according to previous publications.[2,3] Isoprene (Sigma, >99%) was degassed and distilled just before use.

2. CHARACTERISATION

^{1}H- and ^{13}C NMR spectroscopy were performed on a 400 MHz Bruker instrument at 80 °C using a 2:1 mixture of deuterated TCE:C$_6$D$_6$. The chemical shifts (δ) are reported in parts per million (ppm). The conversion of the comonomers **M1** and **M2** was determined according to previous reports.[3,4] The composition of copolymers P(**E**-co-**M1**) was determined by comparing the $\underline{H_3}$C–O– signal of the α-chain ($\int_{2.9}^{3.1} CH_3O$) with the comonomer peaks at 3.96 and 4.4 ppm ($\int_{3.5}^{5.3} CH$ & CH_2) corresponding to the –CH–C$\underline{H_2}$–O(C=O)O–CH$_2$–, –O–C$\underline{H_2}$–CH–CH$_2$(O(C=O)O), –O–CH$_2$–CH–C$\underline{H_2}$(O(C=O)O) and –O–CH$_2$–C$\underline{H}$–CH$_2$(O(C=O)O), respectively, as well as four protons from the oligo-VAc of the initiator ($\int_{4.75}^{5} CH$). The equation to determine the DP of **M1** is

$$DP\ \boldsymbol{M1} = \frac{\int_{3.5}^{5.3} CH\ \&\ CH_2 - \int_{4.75}^{5} CH}{\int_{2.9}^{3.1} CH_3O} \qquad \text{– Equation 1}$$

The DP of ethylene was determined by integrating all the protons from 2.0 to 0.5 ppm ($\int_{0.5}^{2.0} H$; corresponding to 4H of the **E** repeat unit (–C$\underline{H_2}$–) + 39H of the initiating fragment and TEMPO (CH$_3$O–C(C$\underline{H_3}$)$_2$–C$\underline{H_2}$–C(C$\underline{H_3}$)-(CN)–(C$\underline{H_2}$–CH–O–CO–C$\underline{H_3}$)–) and –N–(C(C$\underline{H_3}$)$_2$–(C$\underline{H_2}$)$_3$–C(C$\underline{H_3}$)$_2$) + 3H of the –CH– and –CH$_2$– of **M1** (–C$\underline{H_2}$–C$\underline{H}$–CH$_2$–O–CO–O–). The equation to determine the DP of **E** is

$$DP\ E = \frac{\int_{0.5}^{2.0} H - \frac{39}{3}\int_{2.9}^{3.1} CH_3O - 3\frac{\int_{3.5}^{5.3} CH\ \&\ CH_2 - \int_{4.75}^{5} CH}{\int_{2.9}^{3.1} CH_3O}}{\frac{4}{3}\int_{2.9}^{3.1} CH_3O} \qquad \text{– Equation 2}$$

Size exclusion chromatography (SEC) for ethylene copolymers was performed on a PL-GPC 220 HT Agilent system equipped with 1 guard column and 2 mixed C columns calibrated with poly(styrene) standards, in trichlorobenzene (TCB) stabilised with BHT at 140 °C at a flow rate of 1 mL/min using refractive index detection. For the kinetic investigation, SEC was performed in THF at 45 °C at a flow rate of 1 mL/min with a Viscotek 305 TDA liquid chromatograph equipped with two PSS SDV linear M columns calibrated with polystyrene standards and a refractive index detector.

Fourier-transform infrared analysis (FT-IR) was performed on a ThermoFisher Scientific Nicolet IS5 with module ATR ID5 using a diamond crystal (650 cm^{-1} - 4000 cm^{-1}).

Differential scanning calorimetry (DSC) was performed on a DSC Q100 instrument from TA Instruments by placing around 5 mg of sample in an aluminium pan. The sample was cooled to 0 °C, then heated to 140 °C, cooled to -90 °C and heated to 150 °C at a heating/cooling rate of 10 °C/min. The last heating cycle was used for the determination of the *T*g. Thermogravimetric analysis (TGA) was performed on a TGA Q500 instrument from TA Instruments. Around 5 mg of sample were heated to 100 °C, held there for 10 minutes to remove any remaining solvent and then heated to 600 °C at 20 °C/min

3. COPOLYMERISATION PROCEDURE FOR M1 AND M2

All polymerisations were performed under an inert atmosphere using Schlenk techniques. A typical ethylene copolymerisation aimed at a [**M1**]$_0$/[R-Co(acac)$_2$]$_0$ = 100/1. A solution of R-Co(acac)$_2$ (0.31 mL; 0.118 M stock solution in CH_2Cl_2, 0.037 mmol) was introduced under argon into a purged 30 mL Schlenk tube and evaporated to dryness under reduced pressure at room temperature and 3.69 mL of degassed DMC were added to give solution **A**. In a second 30 mL Schlenk tube, **M1** (0.5 g, 2.5 mmol) was freeze-pumped-thawed thrice to which 2.5 mL of solution A were added using a syringe. This reaction mixture of R-Co(acac)$_2$, **M1** and DMC was then transferred to a previously purged 30 mL stainless steel autoclave (**Figure S1a**) under mild ethylene flux. The pressure was then increased to 50 bar of ethylene and the polymerisation took place at 40°C and 500 rpm. After 24 hrs, aliquots of the reaction mixture were taken for NMR and SEC analyses to determine conversions and the molecular parameters of the polymer, respectively. The reaction mixture was quenched using a degassed solution of TEMPO (150 mg, 1 mmol) in 2 mL of DMC, left to stir for at least 1 hour and then passed over a microsilica column to remove the cobalt using THF. Copolymers which were not soluble in THF were dissolved in hot toluene (65 °C) and the microcolumn was heated as well to keep the polymer soluble. The polymer was then purified by supercritical CO_2 ($scCO_2$) extraction, (see below) according to a previous publication.[4] The resulting pure polymer was then analysed by NMR spectroscopy, FT-IR, DSC, TGA and elemental analyses.

A typical ethylene copolymerisation aimed at a [**M2**]$_0$/[R-Co(acac)$_2$]$_0$ = 100/1. A solution of R- Co(acac)$_2$ (0.95 mL; 0.1182 M stock solution in CH_2Cl_2, 0.112 mmol) was introduced under argon into a purged 30 mL Schlenk tube and evaporated to dryness under reduced pressure at room temperature and 5.6 mL of degassed DMC were added to make up solution **A**. In a second 30 mL Schlenk tube, **M2** (1.2816 g, 10 mmol) was freeze-pumped-thawed thrice to which 5 mL of solution **A** were added using a syringe. This reaction mixture of R-Co(acac)$_2$, **M2** and DMC was then transferred to a previously purged 30 mL stainless steel autoclave (**Figure S1a**) under mild ethylene flux. The pressure was then increased to 50 bar of ethylene and the polymerisation took place at 40°C and 500 rpm. After 24 hrs, aliquots of the reaction mixture were taken for NMR and SEC analyses to determine conversions and the molecular parameters of the polymer, respectively. The reaction mixture was quenched using a degassed solution of TEMPO (150 mg, 1 mmol) in 2 mL of DMC, left to stir for at least 1 hour and then passed over a microsilica column to remove the cobalt using THF. Copolymers which were not soluble in THF were dissolved in hot toluene (65 °C) and the microcolumn was heated as well to keep the polymer soluble. The polymer was then purified by supercritical CO_2 ($scCO_2$) extraction, (see below) according to a previous publication.[4] The resulting pure polymer was then analysed by NMR spectroscopy, FT-IR, DSC, TGA and elemental analyses.

Copolymerisations performed at 500 bar ethylene pressure were performed in a 23 mL autoclave reactor (**Figure S1b**).

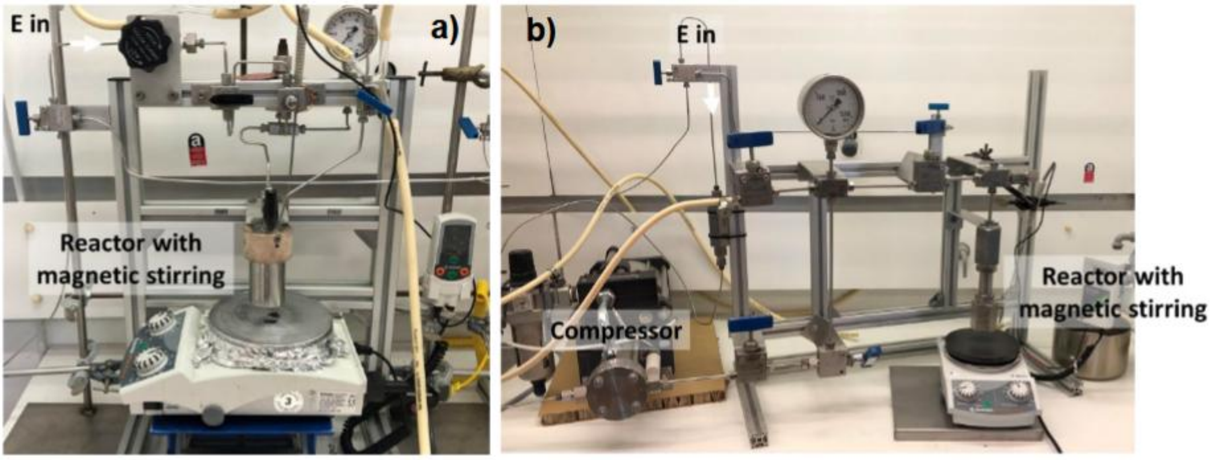

Figure S1. a) The 30 mL autoclave reactor used for ethylene polymerisations at 10, 25, and 50 bar, and b) the 23 mL autoclave reactor used for ethylene polymerisations at 500 bar.

4. COUPLING REACTIONS

The **E/M1** and **E/M2** copolymerisations were performed at 50 bar and 40 °C as described above. After 4 hours of reaction time, the reactor was depressurised and isoprene (1.75 mL, 17.5 mmol) was added to the reaction mixture which was stirred for 2 hours at room temperature. Aliquots for NMR and SEC samples were taken and the polymer purified using $scCO_2$ as described above.

5. SUPERCRITICAL CO_2 EXTRACTION

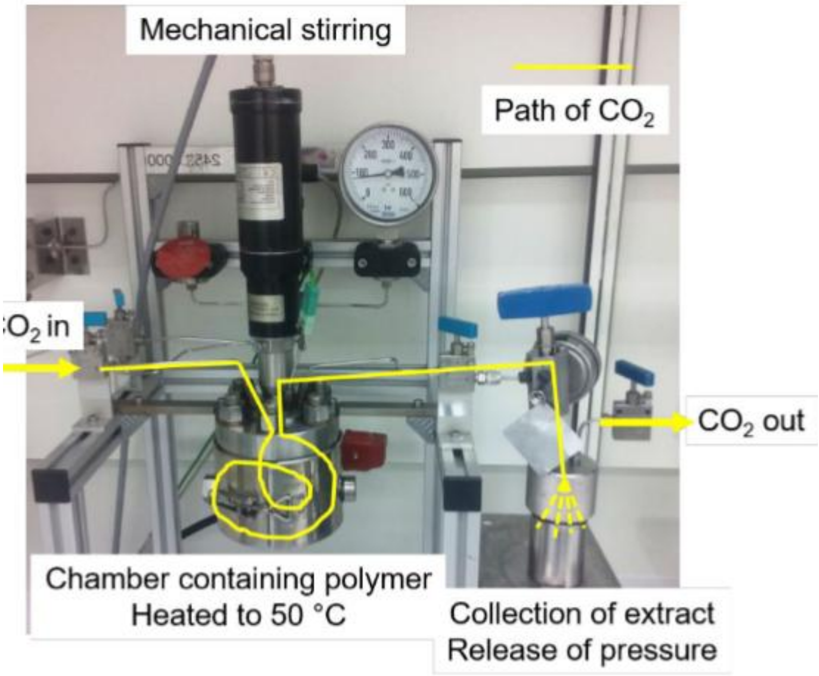

Figure S2. Reactor set-up for the $scCO_2$ extraction of the prepared polymers

The polymer solution was transferred into the main chamber of a $scCO_2$ high pressure reactor (volume of 50 mL, **Figure S2**) which was heated to 50 °C, stirred at 330 rpm and a CO_2 pressure of 250 bar was applied. After 1 hour, the stirring was stopped and $scCO_2$ at 250 bar at a rate of 10 mL/min was flushed through the main chamber and released to atmospheric pressure in another cell connected to the reactor. The unreacted monomers and excess TEMPO were collected in this cell. Once the 250-300 mL of $scCO_2$ were passed through the main chamber, the reactor was vented and the polymer was collected using THF or hot toluene and then dried at 50 °C under vacuum overnight.

An alternative way of purifying this monomer is to use dialysis in THF for **M2** and polymers synthesised at and above 50 bar for **M1**. A 1 kDa regenerated cellulose tubing (Spectrum Labs) was used in this case and the solvent changed twice a day for at least 3 days.

6. COPOLYMERISATION DATA

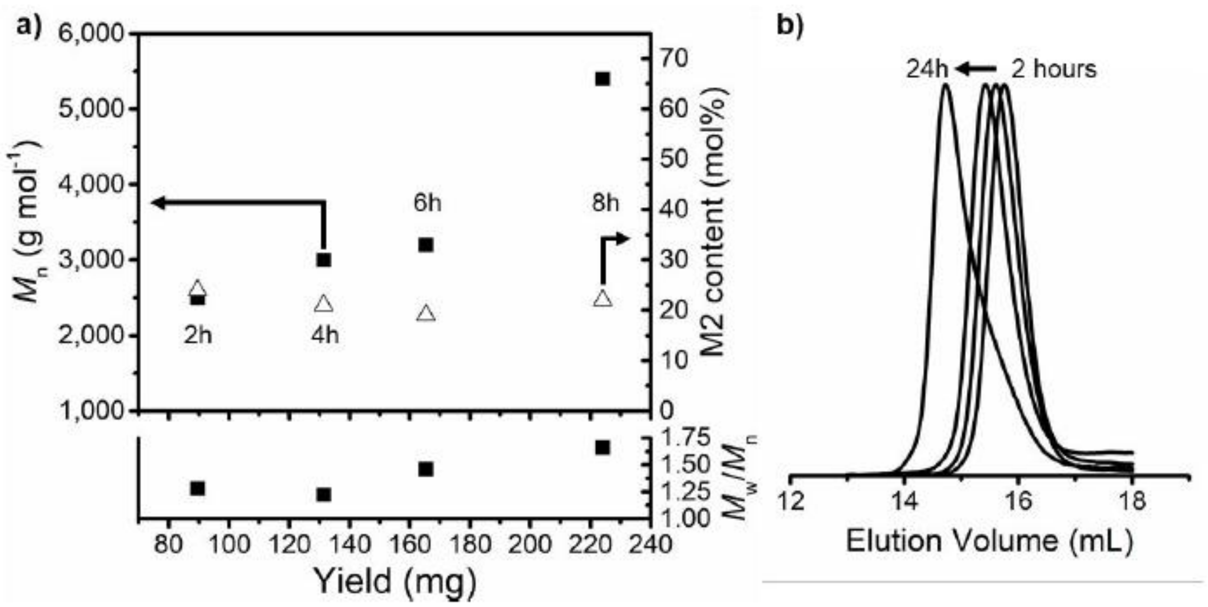

Figure S3. a) Plot of number average molecular weight (M_n), copolymer dispersity and comonomer content (**M2**) against yield at different times for the copolymerisation of ethylene with **M2** using R-Co(acac)$_2$ at 40 °C and 50 bar in DMC, and b) the corresponding size exclusion chromatography (SEC) curves measured at 140 °C in TCB.

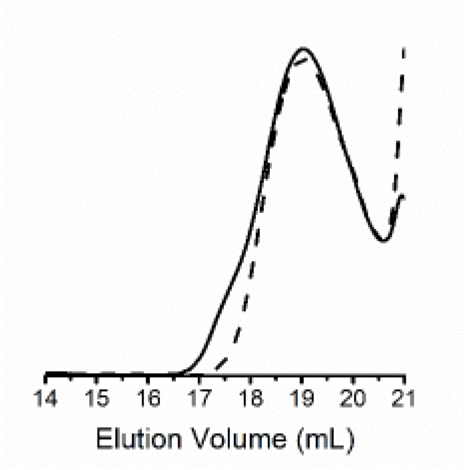

Figure S4. SEC traces of an **E**/**M1** polymerisation before (dashed line) and after (solid line) the addition of isoprene.

In order to give a better appreciation of the yields obtained in the OMRP polymerisations reported in **Tables 1** and **2**, the theoretical maximum yield, i.e. the copolymer yield at 100 % of polar monomer conversion assuming the same copolymer composition, is reported in **Table S1**. An exemplary calculation for entry 3 of **Table S1** is given below.

Table S1: Theoretical maximum yield and yield % calculation for OMRP polymerisations reported in **Table 1** and **2** assuming 100% **M1**/**M2** conversion

Entry	P [a] [bar]	Yield [mg]	X_M [b] [mol%]	Calculated theor. max. yield [mg]	Yield obtained [%]
			M1[c]		
1	10	<10	n.d.	n.d.	n.d.
2	25	32	39	614	5
3	50	72	17	847	8.5
4	500	86	16	872	10
			M2[d]		
5	10	67	62	1,454	5
6	25	163	34	1,826	9
7	50	224	22	2,276	10
8	500	162	10	3,806	4

[a] Ethylene pressure [bar]. [b] X_M = comonomer incorporation (mol%), for **M1** determined by ^{1}H NMR spectroscopy in a 2:1 v/v mixture of TCE:C_6D_6 on a 400 MHz spectrometer at 80 °C using the α–chain end (see **Supporting Information**); for **M2** determined by elemental analysis. [c] Polymerisation conditions: 40 °C, 24 hours, 500 rpm, DMC = 2.5 mL, **M1**/R-Co(acac)$_2$ =100, **M1** = 2.5 mmol = 0.5 g. [d] Polymerisation conditions: 40 °C, 24 hours, 500 rpm, DMC = 5 mL, **M2**/RCo(acac)$_2$ = 100, **M2** = 10 mmol = 1.2816 g.

7. CHARACTERISATION OF THE COPOLYMERS

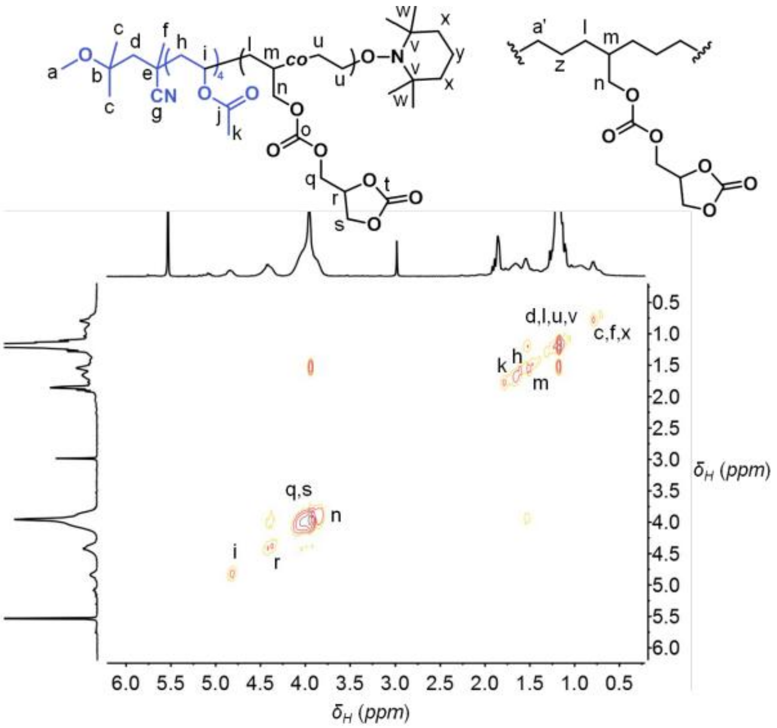

Figure S5. COSY NMR spectrum of P(**E**-*co*-**M1**) (entry 4, **Table 1**) in TCE/C_6D_6 at 80°C.

Published in : ACS Macro Letters (2021), vol. 10, n°03, pp. 313-320
DOI: 10.1021/acsmacrolett.1c000337
Status : Postprint (Author's version)

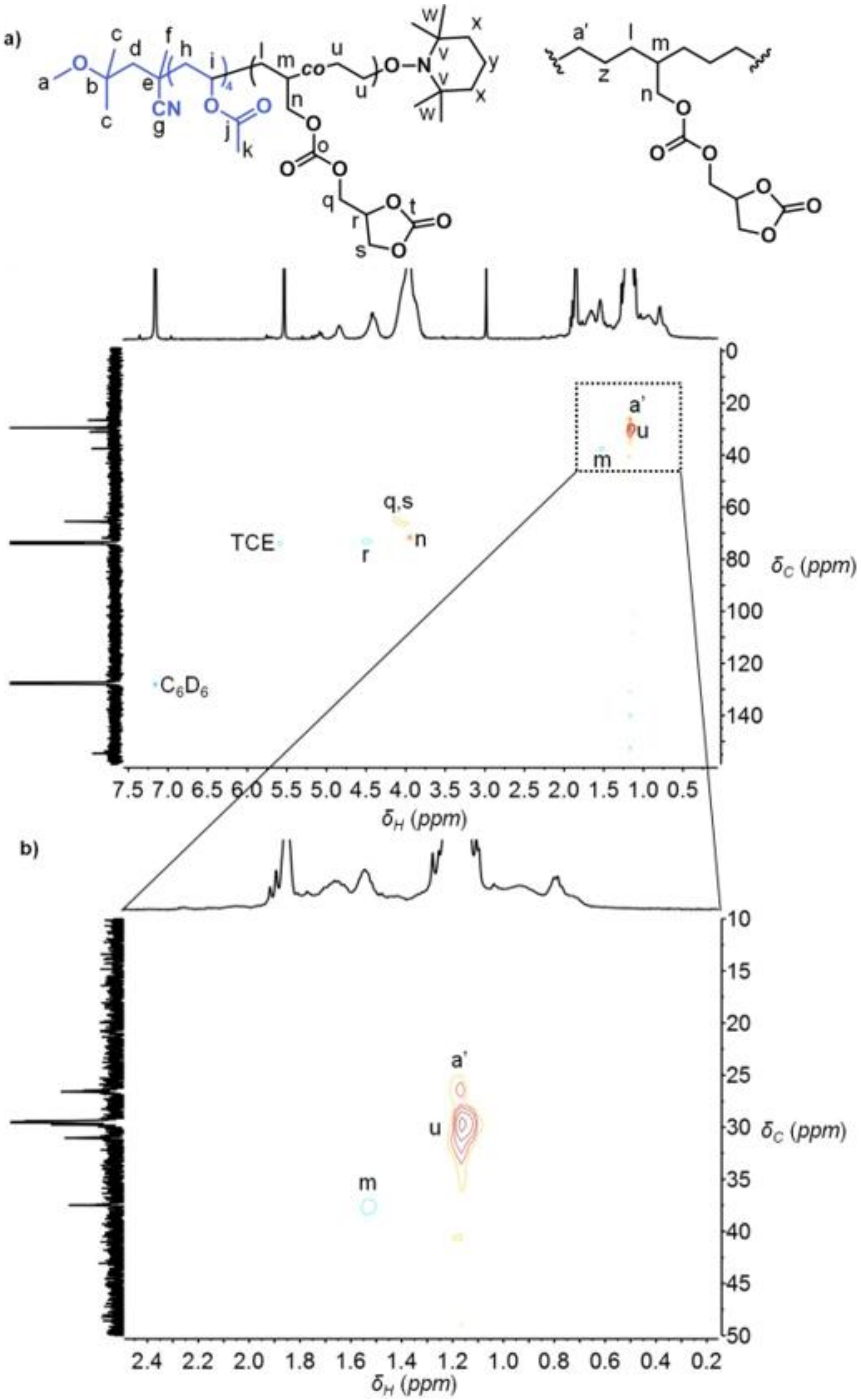

Figure S6. HSQC NMR spectra of P(**E**-*co*-**M1**) (entry 4, **Table 1**) in TCE/C$_6$D$_6$ at 80°C.

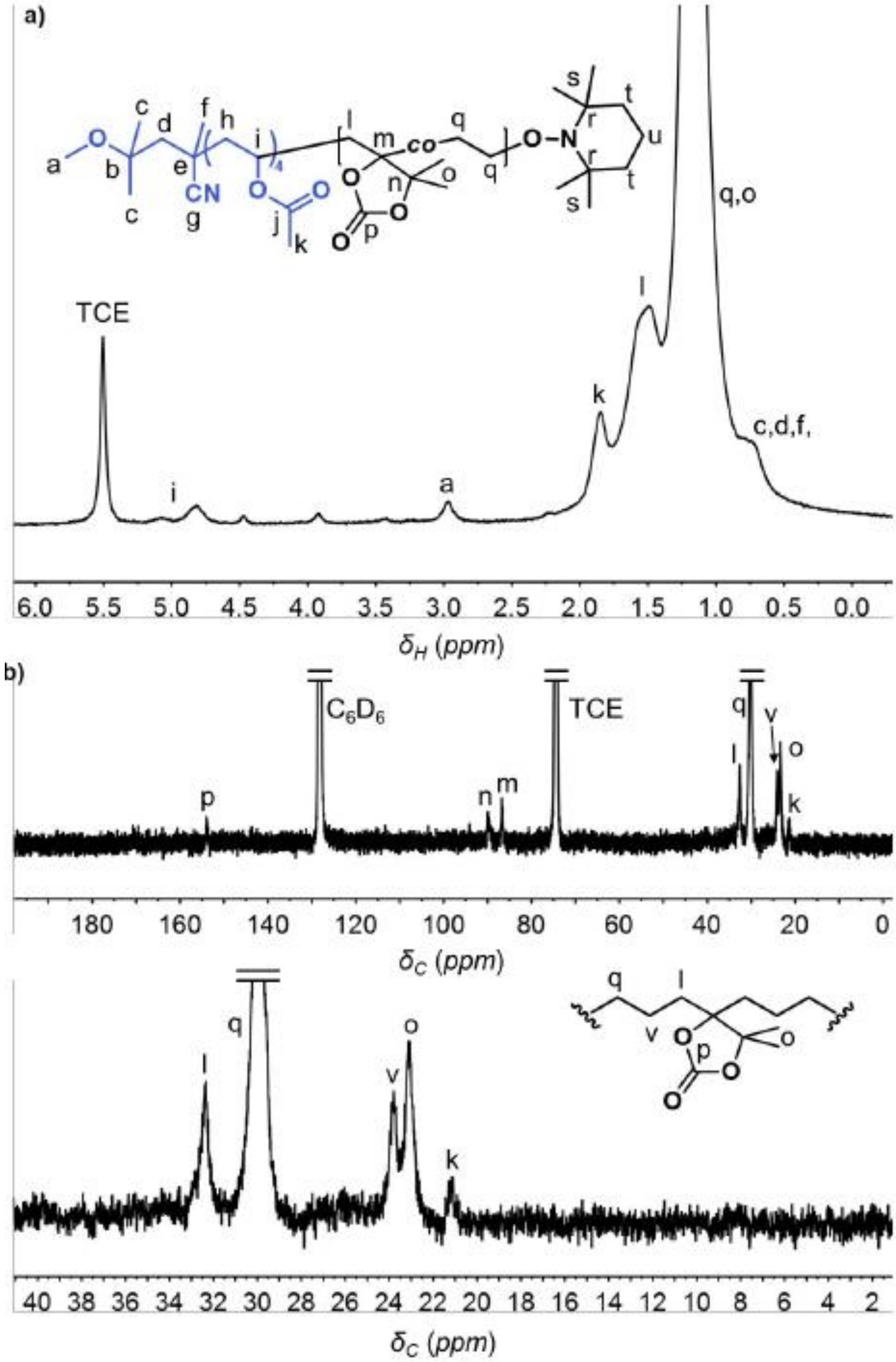

Figure S7. a) 1H- and b) 13C NMR spectra of P(**E**-co-**M2**) (entry 4, **Table 2**) in TCE/C6D6 at 80°C. An inset of the region around 20 ppm where signals from branching would occur is also shown.

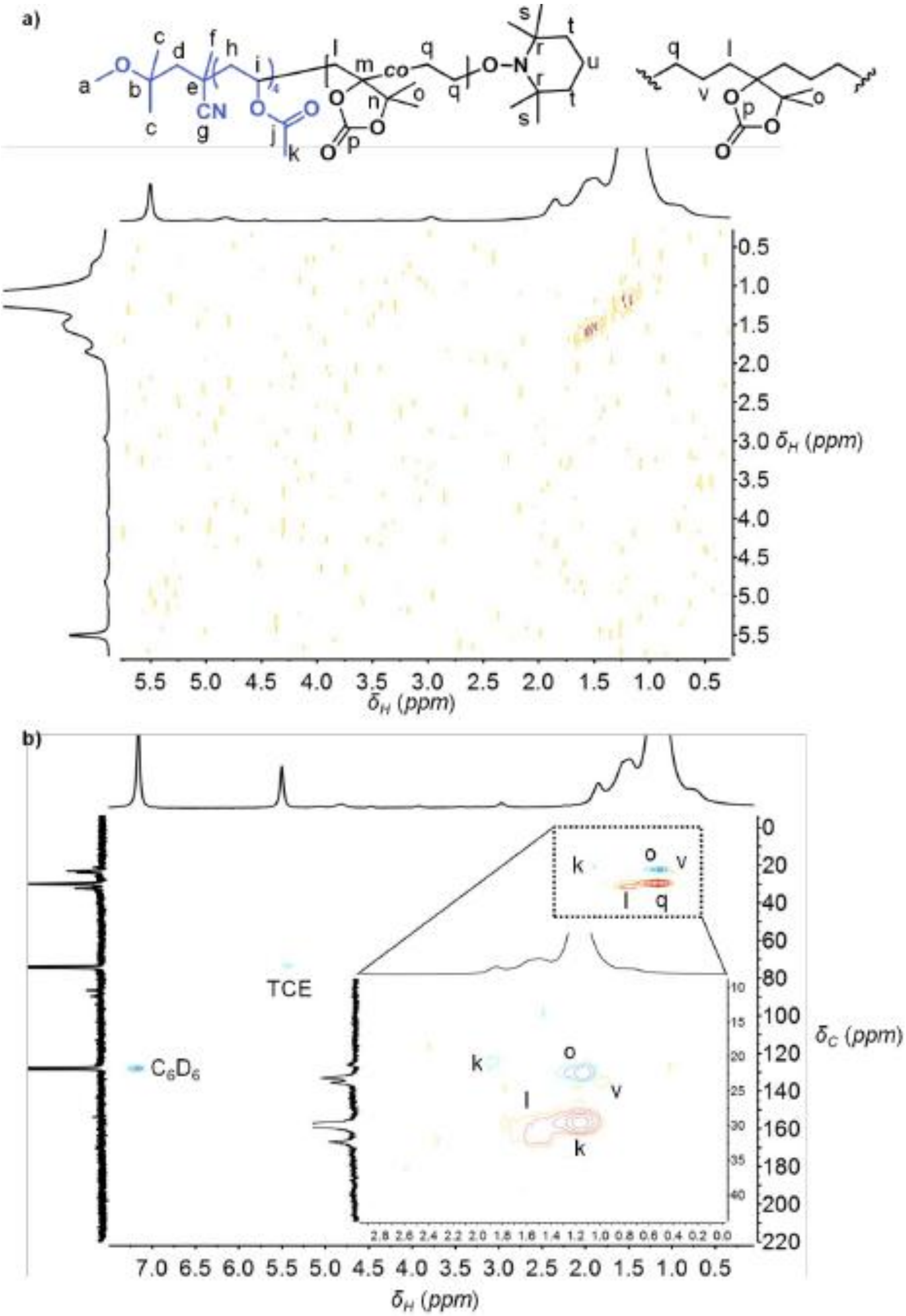

Figure S8. a) COSY and b) HSQC NMR spectra of P(**E**-*co*-**M2**) (entry 4, **Table 2**) in TCE/C_6D_6 at 80°C. An inset of the HSQC spectrum is also shown.

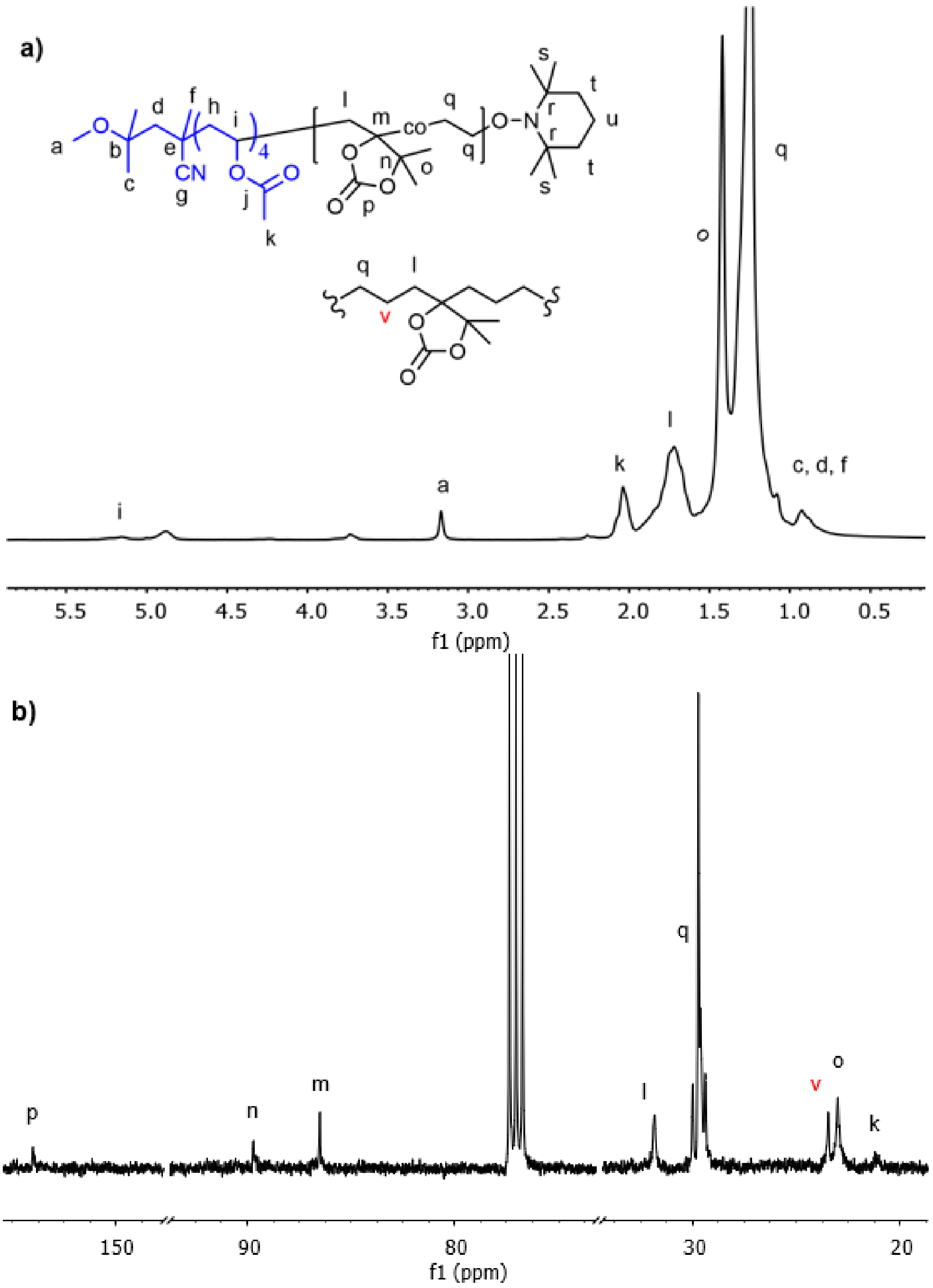

Figure S9. a) ^{1}H- and b) ^{13}C NMR spectra of P(**E**-*co*-**M2**) (entry 4, **Table 2**) in CDCl$_3$ at room temperature.

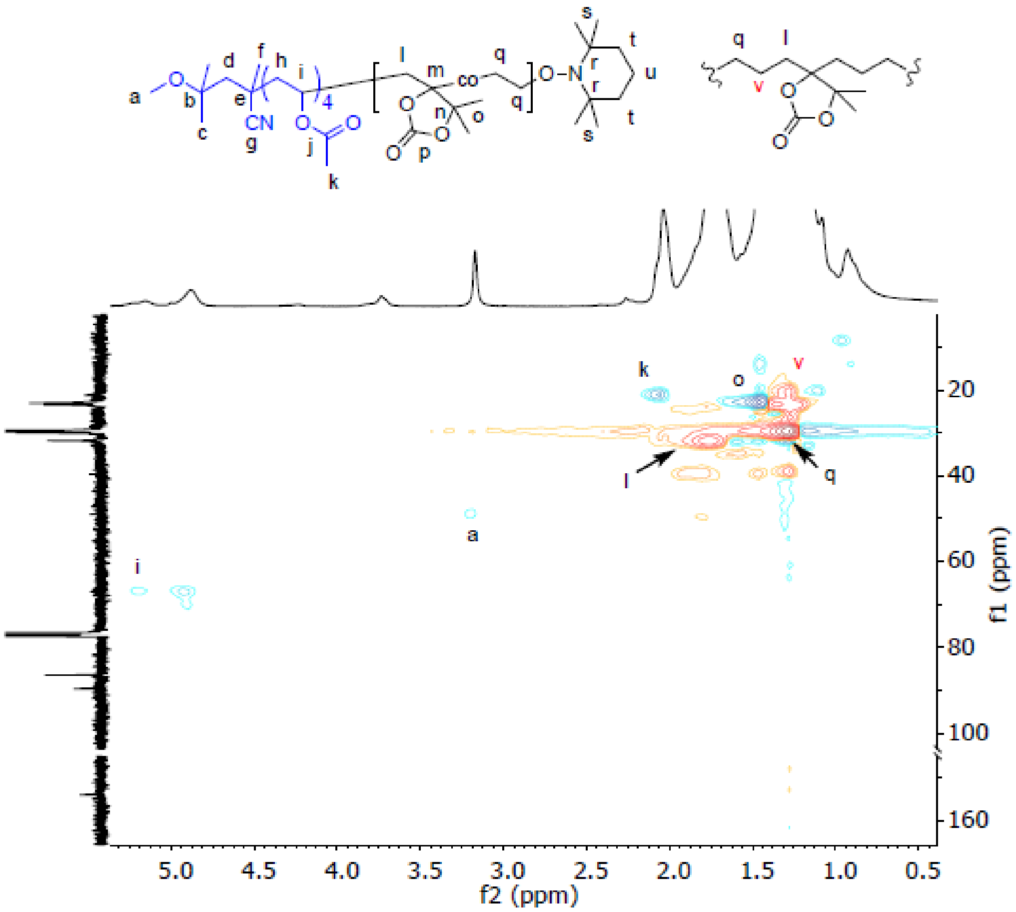

Figure S10. HSQC NMR spectrum of P(**E**-*co*-**M2**) (entry 4, Table 2) in $CDCl_3$ at room temperature.

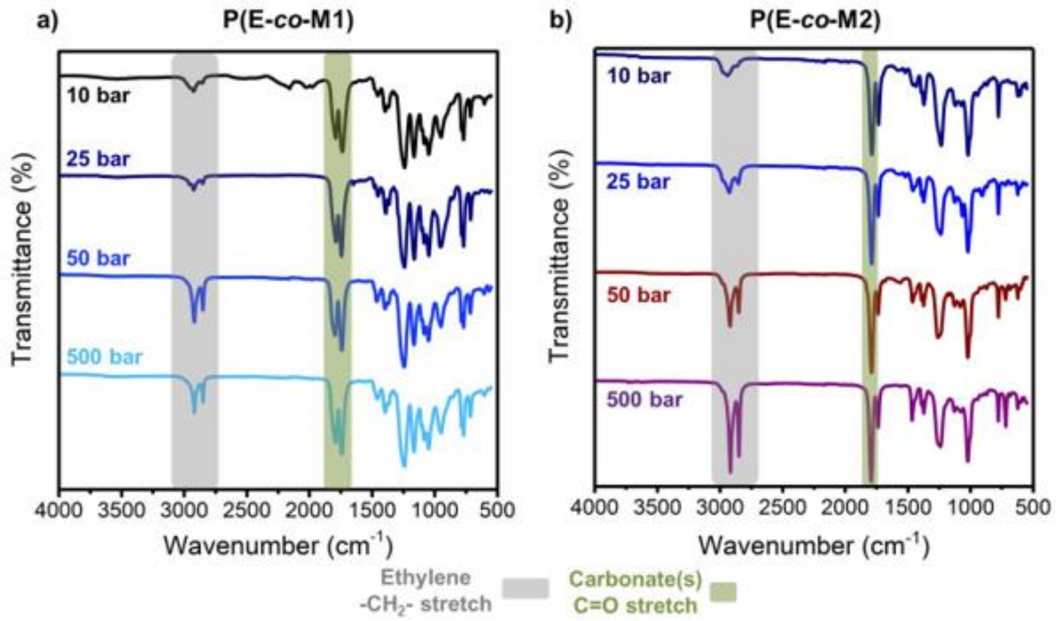

Figure S11. FT-IR spectra of a) P(**M1**-*co*-**E**) copolymers both synthesised at 40 °C in 2.5 mL DMC using R-Co(acac)$_2$, and b) P(**M2**-*co*-**E**) synthesised at 40 °C in 5 mL DMC using RCo(acac)$_2$.

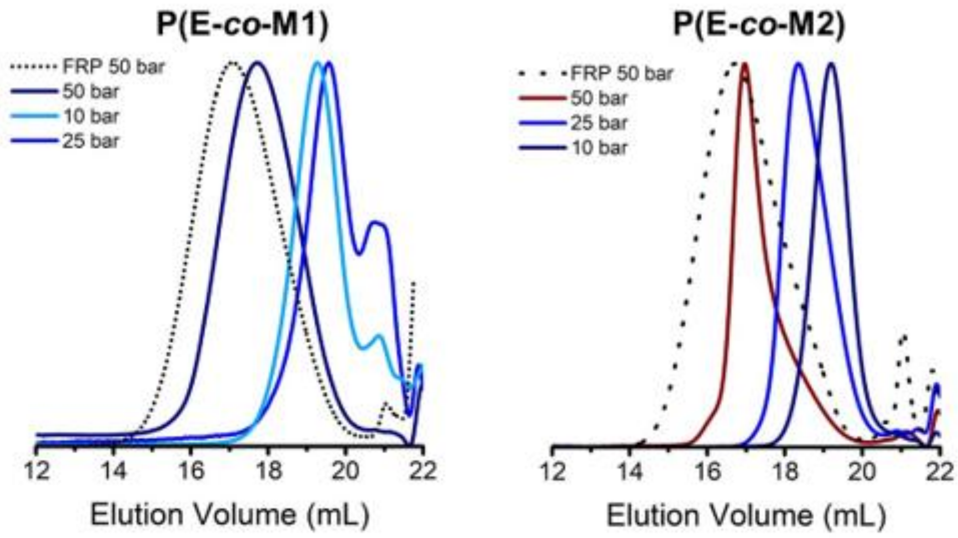

Figure S12. Size-exclusion chromatography (SEC) curves for P(**E**-*co*-**M1**) (**Table 1**) and P(**E**-*co*-**M2**) (**Table 2**) copolymers synthesised at 40 °C in DMC. SEC analyses were performed in THF at 40 °C using a poly(styrene) standard.

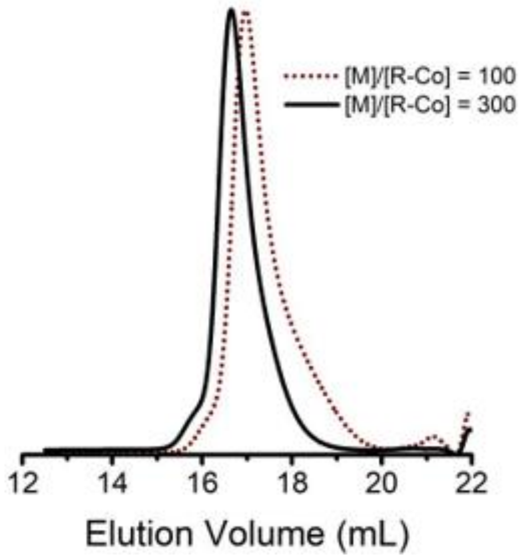

Figure S13. SEC curves performed in THF of P(**E**-co-**M2)** prepared with a [**M2**]/[R-Co] ratio of 100 (dashed wine-coloured line) and 300 (solid black line). Copolymerisation conditions: 50 bar E, **M2** = 10 mmol, 5 mL DMC, 40 °C, 500 rpm, reactor volume = 30 mL. The increase in [**M2**]/[R-Co] ratio increases the average number molecular weights from 8,100 to 14,600 g mol^{-1}, while retaining similar dispersities (1.28 vs. 1.19).

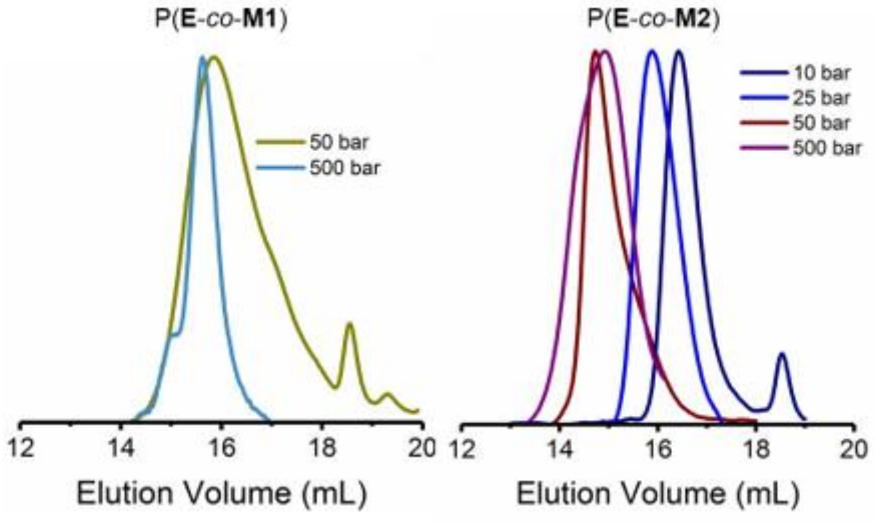

Figure S14. High temperature size-exclusion chromatography (HT-SEC) curves for P(**E**-*co***M1**) (**Table 1**) and P(**E**-*co*-**M2**) (Table 2) copolymers synthesised at 40 °C in DMC. HT-SEC analyses were performed in TCB at 140 °C using a poly(styrene) standard. Note that copolymers P(**E**-*co*-**M1**) synthesised at 10 and 25 bar were not soluble in TCB.

Table S2. Copolymerisations of **E** with **M1** in dimethyl carbonate (DMC) using R-Co(acac)$_2$ [a]. Showing HT-SEC characterisation data

Entry	P [b] [bar]	Yield [mg]	X_M [c] [mol%]	M_n [d] [g mol^{-1}]	$Đ$ [d]	T_g [e] [°C]	T_m [e] [°C]	Cryst [e] [%]
1 [f]	50	56	28	ins.	ins.	n.d.	n.d.	n.d.
2	10	<10	n.d.	n.d.	n.d.	n.d.	n.d.	n.d.
3	25 32 39 ins. ins. -52 - 4 50 72 17 1,300 1.88 5 46 4.5							
5	500	86	16	3,900	1.50	3	108	9.6

[a] Polymerisation conditions: 40 °C, 24 hours, 500 rpm, DMC = 2.5 mL, **M1**/R-Co(acac)$_2$ =100, **M1** = 2.5 mmol. [b] Ethylene pressure [bar]. [c] X_M = comonomer incorporation (mol%), determined by ^{1}H NMR spectroscopy in a 2:1 v/v mixture of TCE:C_6D_6 on a 400 MHz spectrometer at 80 °C using the α–chain end (see **Supporting Information**). [d] Determined using high temperature SEC (HT-SEC) in trichlorobenzene (TCB) at 140 °C using a polystyrene standard. [e] T_g = glass transition temperature (°C), Cryst = copolymer crystallinity (%); determined by differential scanning calorimetry (DSC). Cryst = (ΔH_m measured/$\Delta H_{m\infty}$) × 100, where $\Delta H_{m\infty}$ = 293 J g^{-1}. [f] Use of V70 instead of R-Co(acac)$_2$; V70 = 0.012 mmol, **M1**/R-Co(acac)$_2$ = 100. n.d. = not determined. ins. = insoluble in trichlorobenzene.

Table S3. Copolymerisations of **E** with **M2** in dimethyl carbonate (DMC) using R-Co(acac)$_2$. Showing HT-SEC results for the copolymers

Entry	P [b] [bar]	Yield [mg]	X_M [c] [mol%]	M_n [d] [g mol^{-1}]	Đ [d]	T_g [e] [°C]	T_m [e] [°C]	Cryst [e] [%]
1 [f]	50	67	20	8,400	1.70	n.d.	n.d.	n.d.
2	10	67	62	1,000	1.46	27	-	-
3	25	163	34	1,500	1.63	17	-	-
4	50	224	22	5,400	1.66	2	49	5
5	500	162	10	8,300	1.40	n.o.	90	15

[a] Polymerisation conditions: 40 °C, 24 hours, 500 rpm, DMC = 5 mL, **M2**/R-Co(acac)$_2$ = 100, **M2** = 10 mmol. [b] Ethylene pressure [bar]. [c] X_M = comonomer incorporation (mol%), determined by elemental analysis. [d] Determined using high temperature SEC (HT-SEC) in trichlorobenzene (TCB) at 140 °C using a polystyrene standard. [e] T_g = glass transition temperature (°C), Cryst = copolymer crystallinity (%); determined by differential scanning calorimetry (DSC). Cryst = (ΔH_m measured/$\Delta H_{m\,\infty}$) × 100, where $\Delta H_{m\,\infty}$ = 293 J g^{-1}. [f] Use of V70 instead of R-Co(acac)$_2$; V70 = 0.05 mmol, **M2**/R-Co(acac)$_2$ = 100. n.d. = not determined. n.o. = not observable.

8. DIFFERENTIAL SCANNING CALORIMETRY (DSC) CHARACTERISATION OF THE COPOLYMERS

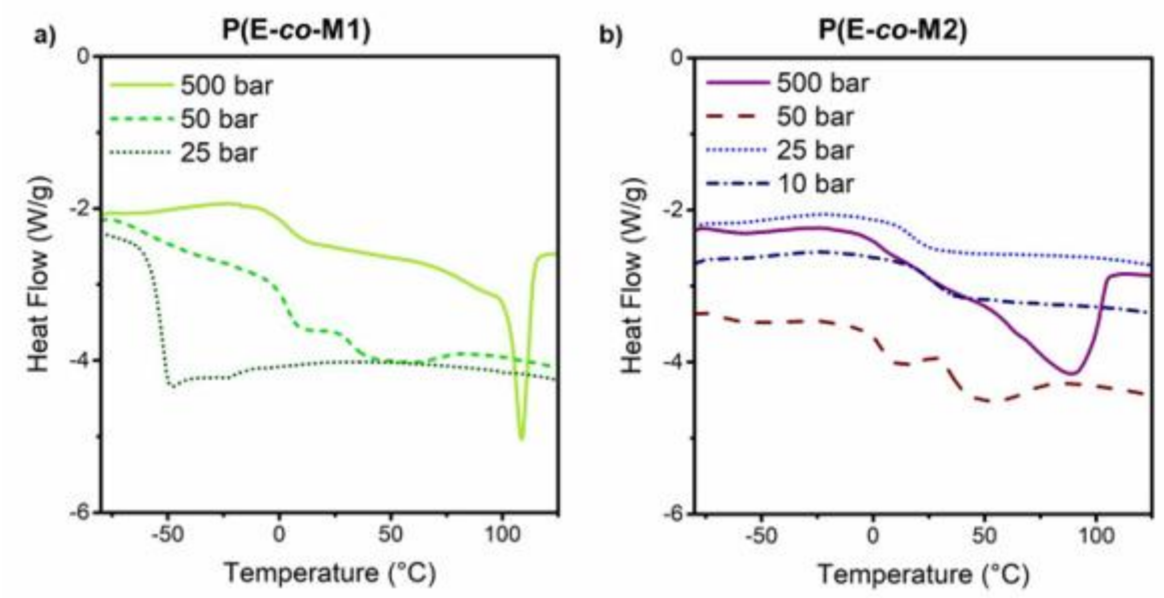

Figure S15. Differential scanning calorimetry (DSC) curves (second heating scan) of a) P(**E***co*-**M1**) and b) P(**E**-*co*-**M2**) synthesised using R-Co(acac)$_2$ at 40 °C at different ethylene pressures.

9. HYDROLYSIS OF P(E-*CO*-M2) AND CHARACTERIZATION

Experimental procedure: in a 50 mL flask, a solution of P(**E**-*co*-M2**)** (0.12 g; Mn = 7,300 g/mol, Đ = 1.15, 18 mol% of **M2**) in ethanol (p.a., 10 mL) was added to an aqueous solution of potassium hydroxide (0.8 g of KOH in 9 mL of water). The mixture was stirred at 75 °C for 32 h under reflux. During the first hours, the copolymer slowly dissolved in the reaction medium with the formation of a homogeneous solution which became turbid after 16 h. After 32 h, ethanol was removed under vacuum, and the aqueous solution of the copolymer was dialyzed for 48 h against water through a Spectra/Pore membrane (molecular weight cut-off: 1000 Da) and then lyophilized, after which the copolymer was recovered as a white powder.

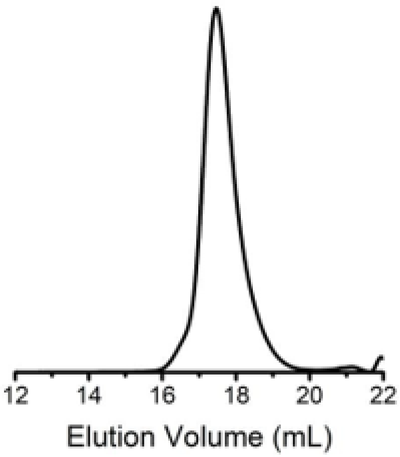

Figure S16. SEC curve in THF of P(**E**-co-**M2**) used for the hydrolysis. Copolymerisation conditions: 50 bar E, **M2** = 10 mmol, 5 mL DMC, 40 °C, 500 rpm, reactor volume = 30 mL. SEC analysis was performed in THF at 40 °C using a poly(styrene) standard.

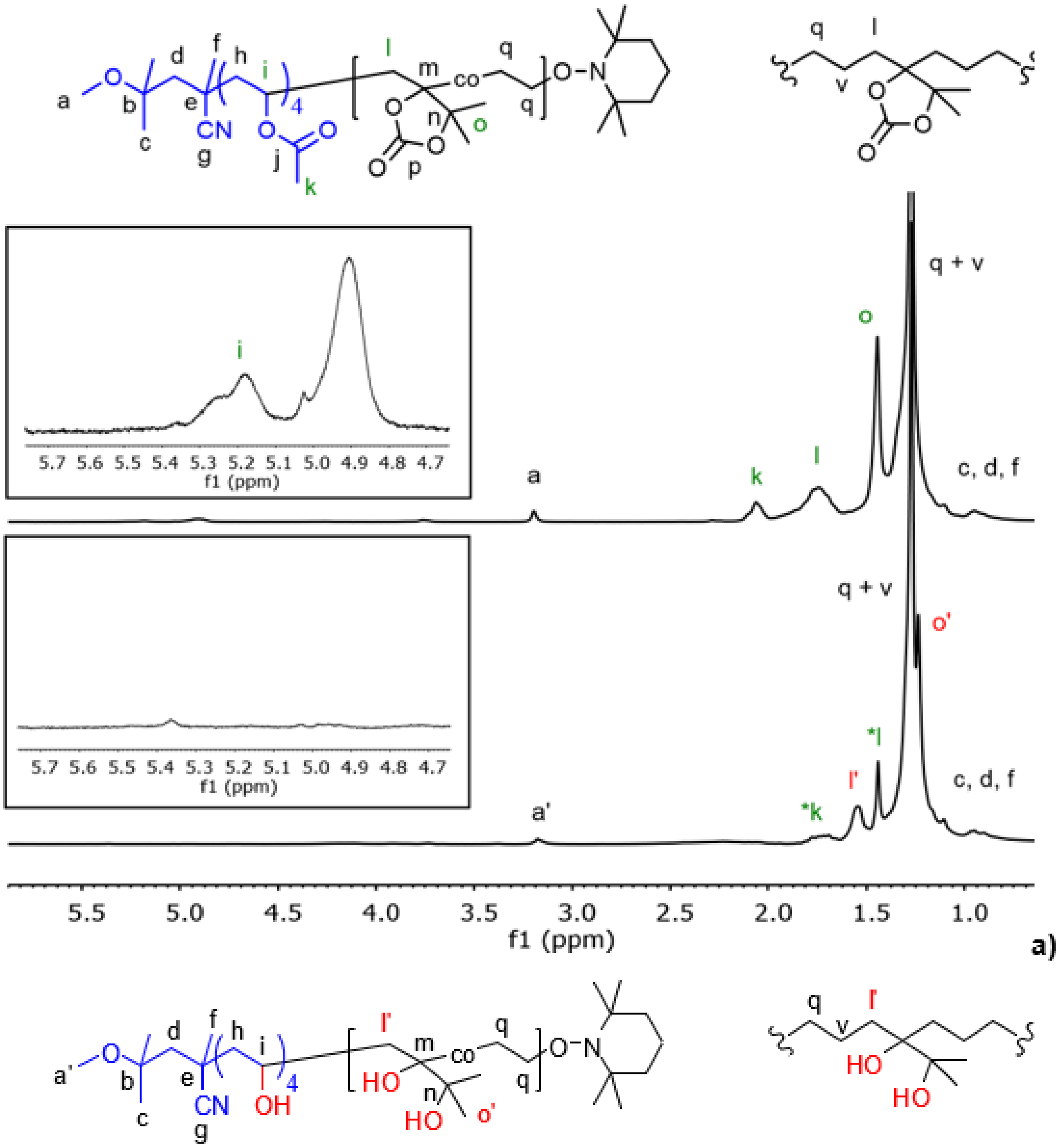

Figure S17. ^{1}H-NMR spectra of P(**E**-*co*-**M2**) copolymer before (top) and after (bottom) hydrolysis. The disappearance of the characteristic acetate (5.2, 4.9, and 2.2 ppm) can be clearly observed while an upfield shift of the CH_2 and CH_3 peaks next to the formed diol repeating unit can be observed in the region of 2-1 ppm. (*k and *l relate to unreacted cyclic carbonate moieties).

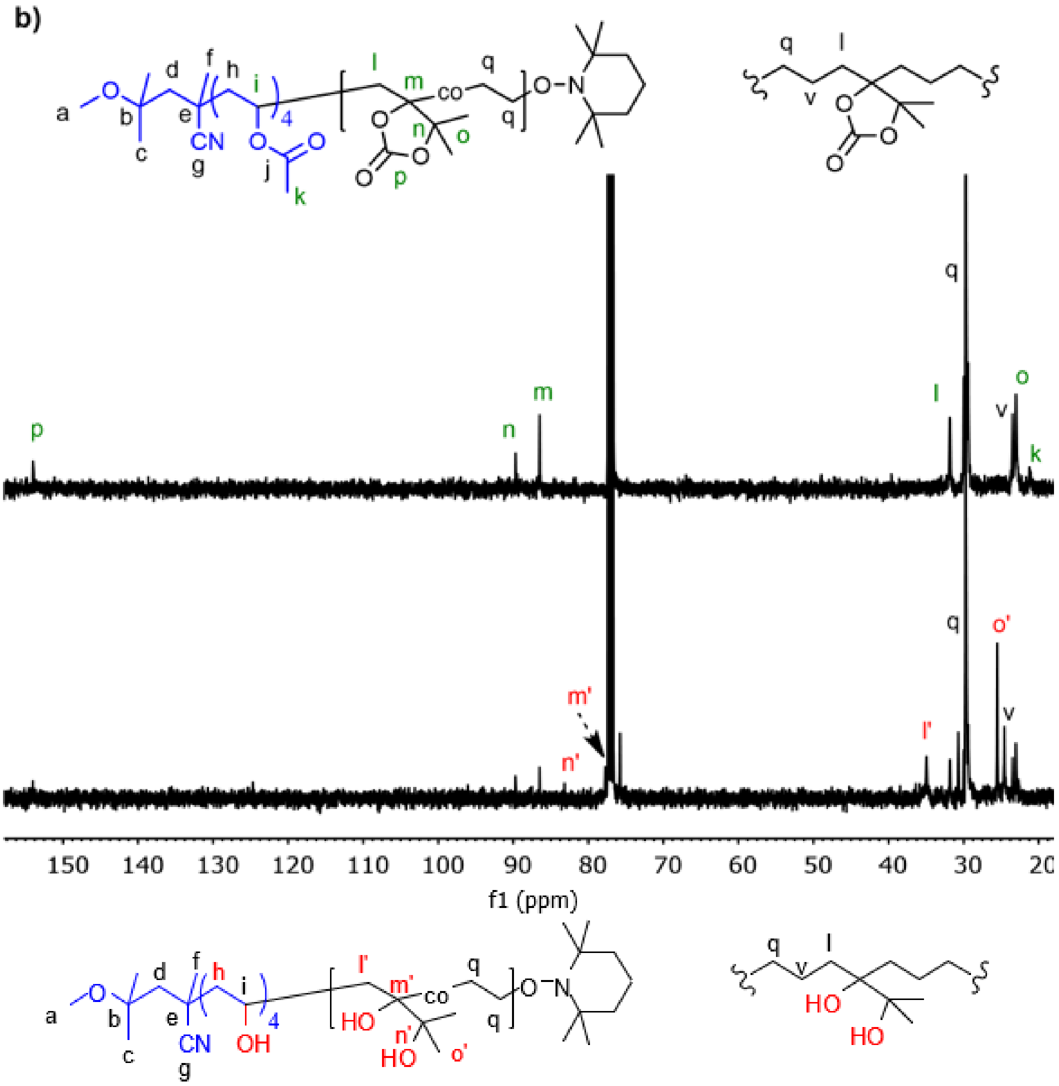

Figure S18. ^{13}C NMR spectra of P(**E**-*co*-**M2**) copolymer before (top) and after (bottom) hydrolysis. The almost complete disappearance of the characteristic carbonate peak at 155 ppm and the upfield shift of the CH_2 and CH_3 peaks next to the formed diol repeating unit can also be observed in the regions of 95-75 ppm and 35-25 ppm.

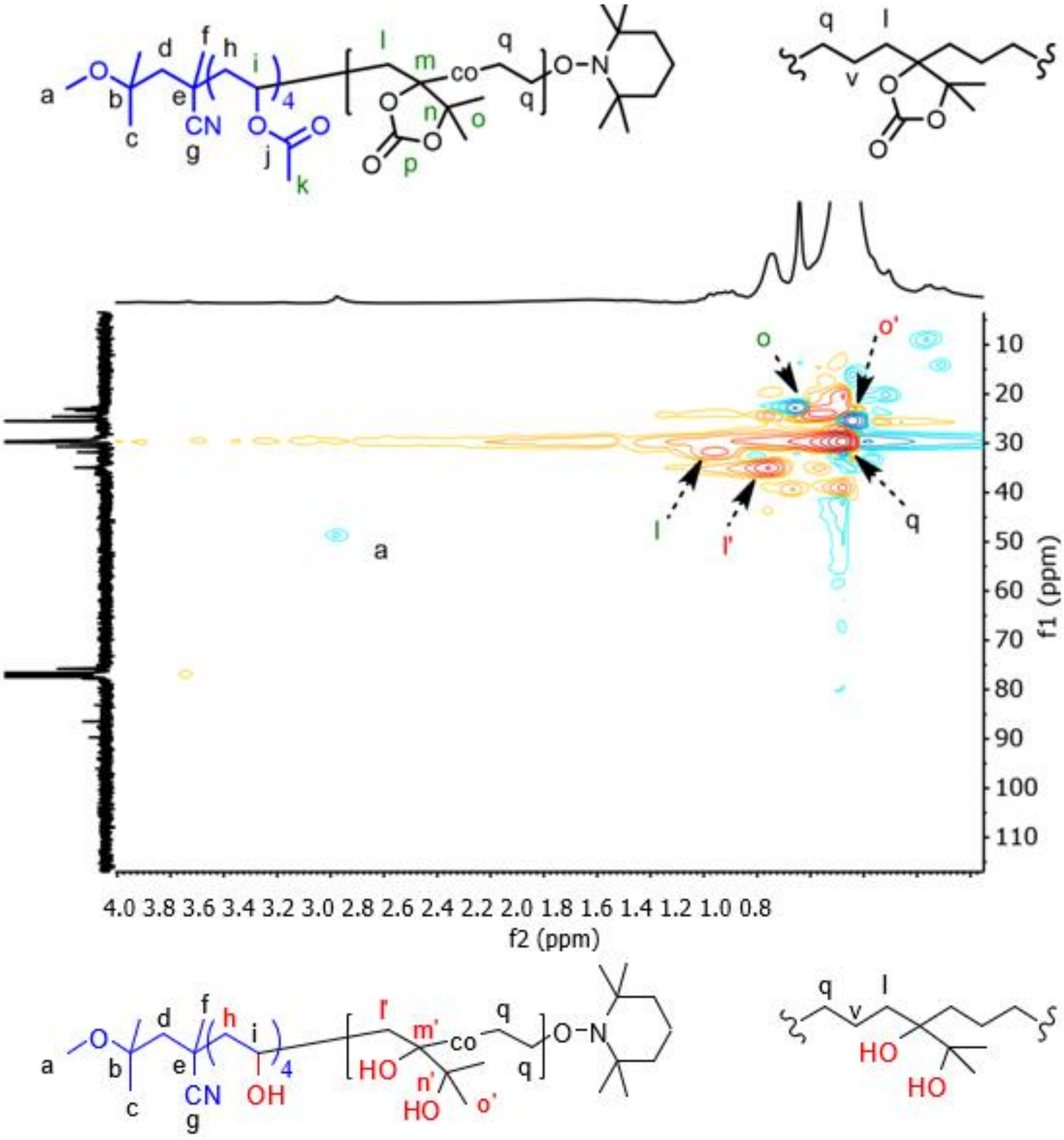

Figure S19. HSQC spectrum of the hydrolysed P(**E**-*co*-**M2**) copolymer in which the presence of both non-hydrolysed (structure on the top) and hydrolysed (structure on the bottom) copolymer can be observed.

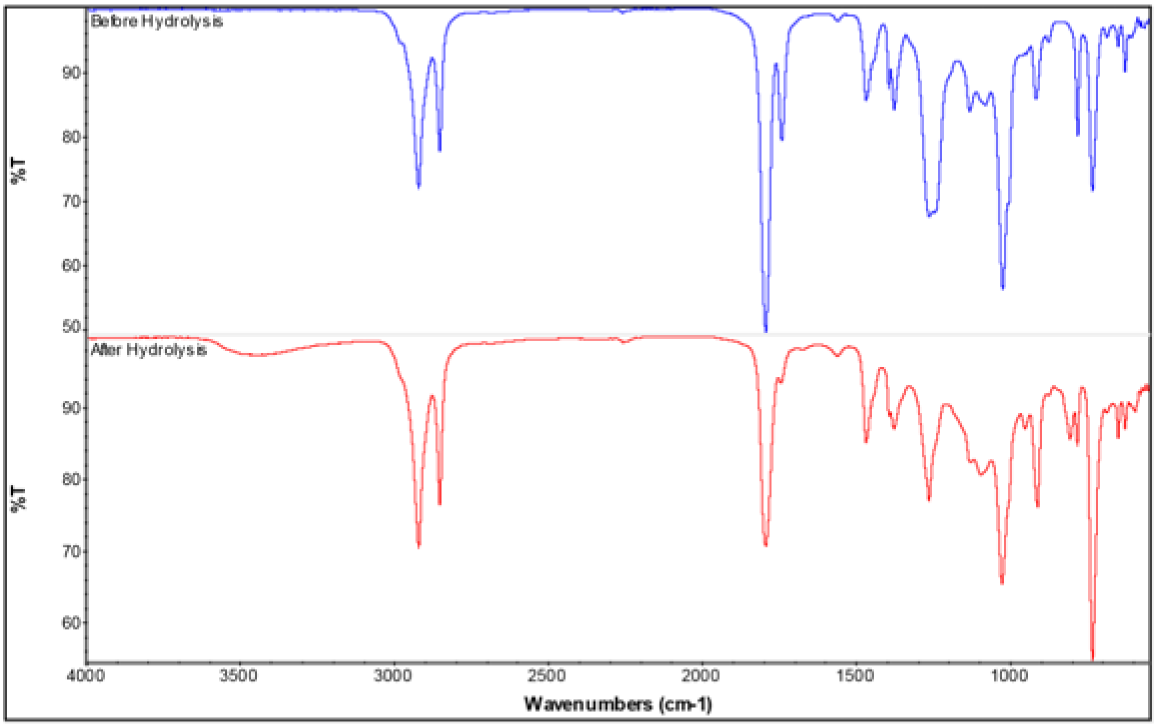

Figure S20. FT-IR spectra of P(**E**-*co*-**M2**) copolymer before and after hydrolysis. The ester (1740 cm^{-1}) and carbonate (1790 cm^{-1}) peak intensities are clearly decreased after the hydrolysis step. In addition, a characteristic OH vibration can be observed at 3450 cm^{-1}. Both confirm the successful hydrolysis which was, however, not complete.

10. REFERENCES

[1] A. Debuigne, Y. Champouret, R. Jérôme, R. Poli, C. Detrembleur, *Chem. - A Eur. J.* **2008**, *14*, 4046–4059.

[2] J. Hu, J. Ma, Q. Zhu, Q. Qian, H. Han, Q. Mei, B. Han, *Green Chem.* **2016**, *18*, 382– 385.

[3] P. B. V. Scholten, J. Demarteau, S. Gennen, J. De Winter, B. Grignard, A. Debuigne, M. A. R. Meier, C. Detrembleur, *Macromolecules* **2018**, *51*, 3379–3393.

[4] P. B. V. Scholten, C. Detrembleur, M. A. R. Meier, *ACS Sustain. Chem. Eng.* **2019**, *7*, 2751–2762.

AUTHOR INFORMATION

CORRESPONDING AUTHORS

Michael A. R. Meier – Institute of Organic Chemistry, Materialwissenschaftliches Zentrum MZE, Karlsruhe Institute of Technology, 76131 Karlsruhe, Germany; Laboratory of Applied Chemistry, Institute of Toxicology and Genetics (ITG), Karlsruhe Institute of Technology (KIT), 76344 Eggenstein-Leopoldshafen, Germany;

Christophe Detrembleur – Center for Education and Research on Macromolecules (CERM), CESAM Research Unit, Department of Chemistry, University of Liège, 4000 Liège, Belgium;

AUTHORS

Philip B. V. Scholten – Center for Education and Research on Macromolecules (CERM), CESAM Research Unit, Department of Chemistry, University of Liège, 4000 Liège, Belgium; Institute of Organic Chemistry, Materialwissenschaftliches Zentrum MZE, Karlsruhe Institute of Technology, 76131 Karlsruhe, Germany;

Grégory Cartigny – Center for Education and Research on Macromolecules (CERM), CESAM Research Unit, Department of Chemistry, University of Liège, 4000 Liège, Belgium

Bruno Grignard – Center for Education and Research on Macromolecules (CERM), CESAM Research Unit, Department of Chemistry, University of Liège, 4000 Liège, Belgium;

Antoine Debuigne – Center for Education and Research on Macromolecules (CERM), CESAM Research Unit, Department of Chemistry, University of Liège, 4000 Liège, Belgium ;

Henri Cramail – Laboratoire de Chimie des Polymères Organiques (LCPO), Université de Bordeaux, 33607 Pessac, France;

AUTHOR CONTRIBUTIONS

All experiments were performed by P.B.V.S and G.C. HT-SEC analysis was performed in the laboratory of H.C. All authors contributed to the manuscript. All authors have given approval to the final version of the manuscript.

NOTES

The authors declare no competing financial interest.

ACKNOWLEDGEMENTS

We thank the European Commission in the framework of the ITN-Marie Curie Program "EJD-FunMat" (grant number 641640). C.D. thanks the "Fonds National pour la Recherche Scientifique" (F.R.S.-FNRS) and the Fonds Wetenschappelijk Onderzoek – Vlaanderen (FWO) for financial support in the frame of the Excellence of Science (EOS) project no. O019618F (ID EOS: 30902231). C.D. is a Research Director and A.D. is a Senior Associate Researcher, both financed by the F.R.S.-FNRS. We also thank Rebecca Seim for her help with the elemental analysis.

REFERENCES

(1) PlasticsEurope. Plastics − the Facts 2018, 2018.

(2) PlasticsEurope. Plastics − the Facts 2019, 2019.

(3) Jeremic, D. Polyethylene. In Ullmann's Encyclopedia of Industrial Chemistry; Wiley-VCH, 2014; pp 1−42.

(4) Braskem. I'm green^{TM} Polyethylene. http://plasticoverde. braskem.com.br/site.aspx/Im-greenTM-Polyethylene (accessed 2019-02-05).

(5) Boffa, L. S.; Novak, B. M. Copolymerization of Polar Monomers with Olefins Using Transition-Metal Complexes. Chem. Rev. 2000, 100 (4), 1479−1493.

(6) Franssen, N. M. G.; Reek, J. N. H.; de Bruin, B. Synthesis of Functional 'Polyolefins': State of the Art and Remaining Challenges. Chem. Soc. Rev. 2013, 42 (13), 5809−5832.

(7) Keyes, A.; Basbug Alhan, H. E.; Ordonez, E.; Ha, U.; Beezer, D. B.; Dau, H.; Liu, Y.-S.; Tsogtgerel, E.; Jones, G. R.; Harth, E. Olefins and Vinyl Polar Monomers: Bridging the Gap for Next Generation Materials. Angew. Chem., Int. Ed. 2019, 58 (36), 12370−12391.

(8) Grignard, B.; Gennen, S.; Jérôme, C.; Kleij, A. W.; Detrembleur, C. Advances in the Use of CO2 as a Renewable Feedstock for the Synthesis of Polymers. Chem. Soc. Rev. 2019, 48 (16), 4466−4514.

(9) Yadav, N.; Seidi, F.; Crespy, D.; D'Elia, V. Polymers Based on Cyclic Carbonates as Trait d'Union Between Polymer Chemistry and Sustainable CO2 Utilization. ChemSusChem 2019, 12 (4), 724−754. (10) Cai, A.; Guo, W.; Martínez-Rodríguez, L.; Kleij, A. W. Palladium-Catalyzed Regio- and Enantioselective Synthesis of Allylic Amines Featuring Tetrasubstituted Tertiary Carbons. J. Am. Chem. Soc. 2016, 138 (43), 14194−14197.

(11) Sopeña, S.; Laserna, V.; Guo, W.; Martin, E.; Escudero-Adan, É. C.; Kleij, A. W. Regioselective Organocatalytic Formation of Carbamates from Substituted Cyclic Carbonates. Adv. Synth. Catal. 2016, 358 (14), 2172−2178.

(12) Scholten, P. B. V.; Demarteau, J.; Gennen, S.; De Winter, J.; Grignard, B.; Debuigne, A.; Meier, M. A. R.; Detrembleur, C. Merging CO2-Based Building Blocks with Cobalt-Mediated Radical Polymerization for the Synthesis of Functional Poly(Vinyl Alcohol)S. Macromolecules 2018, 51 (9), 3379−3393.

(13) Cornille, A.; Blain, M.; Auvergne, R.; Andrioletti, B.; Boutevin, B.; Caillol, S. A Study of Cyclic Carbonate Aminolysis at Room Temperature: Effect of Cyclic Carbonate Structures and Solvents on Polyhydroxyurethane Synthesis. Polym. Chem. 2017, 8 (3), 592−604.

(14) Blain, M.; Jean-Gérard, L.; Auvergne, R.; Benazet, D.; Caillol, S.; Andrioletti, B. Rational Investigations in the Ring Opening of Cyclic Carbonates by Amines. Green Chem. 2014, 16 (9), 4286−4291. (15) Olsén, P.; Oschmann, M.; Johnston, E. V.; Åkermark, B. Synthesis of Highly Functional Carbamates through Ring-Opening of Cyclic Carbonates with Unprotected α-Amino Acids in Water. Green Chem. 2018, 20 (2), 469−475.

(16) Liu, D.; Thomas, T.; Gong, H.; Li, F.; Li, Q.; Song, L.; Azhagan, T.; Jiang, H.; Yang, M. A Mechanism of Alkali Metal Carbonates Catalysing the Synthesis of β-Hydroxyethyl Sulfide with Mercaptan and Ethylene Carbonate. Org. Biomol. Chem. 2019, 17 (42), 9367−9374.

(17) Alves, M.; Grignard, B.; Mereau, R.; Jerome, C.; Tassaing, T.; Detrembleur, C. Organocatalyzed Coupling of Carbon Dioxide with Epoxides for the Synthesis of Cyclic Carbonates: Catalyst Design and Mechanistic Studies. Catal. Sci. Technol. 2017, 7 (13), 2651−2684.

(18) Martín, C.; Fiorani, G.; Kleij, A. W. Recent Advances in the Catalytic Preparation of Cyclic Organic Carbonates. ACS Catal. 2015, 5 (2), 1353−1370.

(19) Fiorani, G.; Guo, W.; Kleij, A. W. Sustainable Conversion of Carbon Dioxide: The Advent of Organocatalysis. Green Chem. 2015, 17 (3), 1375−1389.

(20) Büttner, H.; Longwitz, L.; Steinbauer, J.; Wulf, C.; Werner, T. Recent Developments in the Synthesis of Cyclic Carbonates from Epoxides and CO_2. Top. Curr. Chem. 2017, 375 (3), 50.

(21) Shaikh, R. R.; Pornpraprom, S.; D'Elia, V. Catalytic Strategies for the Cycloaddition of Pure, Diluted, and Waste CO2 to Epoxides under Ambient Conditions. ACS Catal. 2018, 8 (1), 419−450.

(22) Dalpozzo, R.; Della Ca', N.; Gabriele, B.; Mancuso, R. Recent Advances in the Chemical Fixation of Carbon Dioxide: A Green Route to Carbonylated Heterocycle Synthesis. Catalysts 2019, 9 (6), 511.

(23) Dabral, S.; Schaub, T. The Use of Carbon Dioxide (CO_2) as a Building Block in Organic Synthesis from an Industrial Perspective. Adv. Synth. Catal. 2019, 361 (2), 223−246.

(24) Peña Carrodeguas, L.; Cristofol, À`.; Fraile, J. M.; Mayoral, J. A.; Dorado, V.; Herrerías, C. I.; Kleij, A. W. Fatty Acid Based Biocarbonates: Al-Mediated Stereoselective Preparation of Mono-, Di- and Tricarbonates under Mild and Solvent-Less Conditions. Green Chem. 2017, 19 (15), 3535−3541.

(25) Tenhumberg, N.; Büttner, H.; Schaffner̈, B.; Kruse, D.; Blumenstein, M.; Werner, T. Cooperative Catalyst System for the Synthesis of Oleochemical Cyclic Carbonates from CO_2 and Renewables. Green Chem. 2016, 18 (13), 3775−3788.

(26) Cho, I.; Lee, T. Radical Polymerization of 4-Methylene-l,3Dioxolan-2-One and Its Hydrolyzed Water-Soluble Polymer. Makromol. Chem., Rapid Commun. 1989, 10, 453−456.

(27) Ochiai, B.; Sano, Y.; Endo, T. Synthesis and Crosslinking of Oligo(Carbonate-Ketone) Obtained by Radical Polymerization of 4Methylene-5,5-Dimethyl-1,3-Dioxolan-2-One. J. Netw. Polym. Japan 2005, 26 (3), 132−137.

(28) Liu, B.; Zhang, Y.; Zhang, X.; Du, B.; Fan, Z. Fixation of Carbon Dioxide Concurrently or Tandem with Free Radical Polymerization for Highly Transparent Polyacrylates with Specific UV Absorption. Polym. Chem. 2016, 7 (22), 3731−3739.

(29) Tale, N. V.; Jagtap, R. N.; Tathe, D. S. An Efficient Approach for the Synthesis of Thermoset Polyurethane Acrylate Polymer and Its Film Properties. Des. Monomers Polym. 2014, 17 (2), 147−155.

(30) Jana, S.; Yu, H.; Parthiban, A.; Chai, C. L. L. Controlled Synthesis and Functionalization of PEGylated Methacrylates Bearing Cyclic Carbonate Pendant Groups. J. Polym. Sci., Part A: Polym. Chem. 2010, 48 (7), 1622−1632.

(31) Palaskar, D. V.; Sane, P. S.; Wadgaonkar, P. P. A New ATRP Initiator for Synthesis of Cyclic Carbonate-Terminated Poly(Methyl Methacrylate). React. Funct. Polym. 2010, 70 (12), 931−937.

(32) Scholten, P. B. V.; Detrembleur, C.; Meier, M. A. R. Plant-Based Non-Activated Olefins: A New Class of Renewable Monomers for Controlled Radical Polymerisation. ACS Sustainable Chem. Eng. 2019, 7 (2), 2751−2762.

(33) Laible, R. C. Allyl Polymerizations. Chem. Rev. 1958, 58 (5), 807−843.

(34) Bartlett, P. D.; Altschul, R. The Polymerization of Allyl Compounds. I. Factors Governing the Acyl Peroxide-Induced Polymerization of Allyl Acetate, and the Fate of the Peroxide. J. Am. Chem. Soc. 1945, 67 (5), 812−816.

(35) Bartlett, P. D.; Altschul, R. The Polymerization of Allyl Compounds. II. Preliminary Kinetic Study of the Peroxide-Induced Polymerization of Allyl Acetate. J. Am. Chem. Soc. 1945, 67 (5), 816− 822.

(36) Bartlett, P. D.; Nozaki, K. The Polymerization of Allyl Compounds. III. The Peroxide-Induced Copolymerization of Allyl Acetate with Maleic Anhydride. J. Am. Chem. Soc. 1946, 68 (8), 1495−1504.

(37) Bartlett, P. D.; Tate, F. A. The Polymerization of Allyl Compounds. VI. The Polymerization of Allyl-1-D2 Acetate and the Mechanism of Its Chain Termination. J. Am. Chem. Soc. 1953, 75 (1), 91−95.

(38) Kermagoret, A.; Debuigne, A.; Jérôme, C.; Detrembleur, C. Precision Design of Ethylene- and Polar-Monomer-Based Copolymers by Organometallic-Mediated Radical Polymerization. Nat. Chem. 2014, 6 (3), 179−187.

(39) Dommanget, C.; D'Agosto, F.; Monteil, V. Polymerization of Ethylene through Reversible Addition-Fragmentation Chain Transfer (RAFT). Angew. Chem., Int. Ed. 2014, 53 (26), 6683−6686.

(40) Chen, Q. B.; Zeng, T. Y.; Xia, L.; Zhang, Z.; Hong, C. Y.; Zou, G.; You, Y. Z. A RAFT/MADIX Method Finely Regulating the Copolymerization of Ethylene and Polar Vinyl Monomers under Mild Conditions. Chem. Commun. 2017, 53 (78), 10780−10783.

(41) Demarteau, J.; Kermagoret, A.; Jérôme, C.; Detrembleur, C.; Debuigne, A. Controlled Synthesis of Ethylene-Vinyl Acetate Based Copolymers by Organometallic Mediated Radical Polymerization. ACS Symp. Ser. 2015, 1188, 47−61.

(42) Zeng, T.; You, W.; Chen, G.; Nie, X.; Zhang, Z.; Xia, L.; Hong, C.; Chen, C.; You, Y. Degradable PE-Based Copolymer with Controlled Ester Structure Incorporation by Cobalt-Mediated Radical Copolymerization under Mild Condition. iScience 2020, 23 (3), 100904.

(43) Wolpers, A.; Baffie, F.; Verrieux, L.; Perrin, L.; Monteil, V.; D'Agosto, F. Iodine-Transfer Polymerization (ITP) of Ethylene and Copolymerization with Vinyl Acetate. Angew. Chem., Int. Ed. 2020, 59 (43), 19304−19310.

(44) Demarteau, J.; De Winter, J.; Detrembleur, C.; Debuigne, A. Ethylene/Vinyl Acetate-Based Macrocycles via Organometallic-Mediated Radical Polymerization and CuAAC "click" Reaction. Polym. Chem. 2018, 9 (3), 273−278.

(45) Boyaval, A.; Méreau, R.; Grignard, B.; Detrembleur, C.; Jerome, C.; Tassaing, T. Organocatalytic Coupling of CO2 with a Propargylic Alcohol: A Comprehensive Mechanistic Study. ChemSusChem 2017, 10 (6), 1241−1248.

(46) Debuigne, A.; Jérôme, C.; Detrembleur, C. Organometallic-Mediated Radical Polymerization of 'Less Activated Monomers': Fundamentals, Challenges and Opportunities. Polymer 2017, 115, 285−307.

(47) Roedel, J. M. The Molecular Structure of Polyethylene. I. Chain Branching in Polyethylene during Polymerization. J. Am. Chem. Soc. 1953, 75 (24), 6110−6112.

(48) Matsumoto, A. Polymerization of Multiallyl Monomers. Prog. Polym. Sci. 2001, 26 (2), 189−257.

(49) Inoue, S.; Tamezawa, H.; Aota, H.; Matsumoto, A.; Yokoyama, K.; Matoba, Y.; Shibano, M. Addition-Fragmentation Chain Transfer in Allyl Polymerization at Elevated Temperatures. Macromolecules 2011, 44 (8), 3169−3173.

(50) Demarteau, J.; Scholten, P. B. V.; Kermagoret, A.; De Winter, J.; Meier, M. A. R.; Monteil, V.; Debuigne, A.; Detrembleur, C. Functional Polyethylene (PE) and PE-Based Block Copolymers by Organometallic-Mediated Radical Polymerization´. Macromolecules 2019, 52 (22), 9053−9063.

(51) Grau, E.; Broyer, J. P.; Boisson, C.; Spitz, R.; Monteil, V. Unusual Activation by Solvent of the Ethylene Free Radical Polymerization. Polym. Chem. 2011, 2 (10), 2328−2333.

(52) Dai, S.; Chen, C. Palladium-Catalyzed Direct Synthesis of Various Branched, Carboxylic Acid-Functionalized Polyolefins: Characterization, Derivatization, and Properties. Macromolecules 2018, 51 (17), 6818−6824.

(53) Dai, S.; Chen, C. Direct Synthesis of Functionalized High-Molecular-Weight Polyethylene by Copolymerization of Ethylene with Polar Monomers. Angew. Chem., Int. Ed. 2016, 55 (42), 13281− 13285.

(54) Zou, C.; Dai, S.; Chen, C. Ethylene Polymerization and Copolymerization Using Nickel 2-Iminopyridine-N-Oxide Catalysts: Modulation of Polymer Molecular Weights and Molecular-Weight Distributions. Macromolecules 2018, 51 (1), 49−56.

(55) Yasuda, H.; Nakano, R.; Ito, S.; Nozaki, K. Palladium/IzQOCatalyzed Coordination − Insertion Copolymerization of Ethylene and 1,1-Disubstituted Ethylenes Bearing a Polar Functional Group. J. Am. Chem. Soc. 2018, 140 (5), 1876−1883.

(56) Wang, X.; Nozaki, K. Selective Chain-End Functionalization of Polar Polyethylenes: Orthogonal Reactivity of Carbene and Polar Vinyl Monomers in Their Copolymerization with Ethylene. J. Am. Chem. Soc. 2018, 140 (46), 15635−15640.

(57) Mitsushige, Y.; Yasuda, H.; Carrow, B. P.; Ito, S.; Kobayashi, M.; Tayano, T.; Watanabe, Y.; Okuno, Y.; Hayashi, S.; Kuroda, J.; Okumura, Y.; Nozaki, K. Methylene-Bridged Bisphosphine Monoxide Ligands for Palladium-Catalyzed Copolymerization of Ethylene and Polar Monomers. ACS Macro Lett. 2018, 7 (3), 305−311.

(58) Na, Y.; Dai, S.; Chen, C. Direct Synthesis of Polar-Functionalized Linear Low-Density Polyethylene (LLDPE) and Low-Density Polyethylene (LDPE). Macromolecules 2018, 51, 4040−4048.

(59) Jung, J.; Yasuda, H.; Nozaki, K. Copolymerization of Nonpolar Olefins and Allyl Acetate Using Nickel Catalysts Bearing a Methylene-Bridged Bisphosphine Monoxide Ligand. Macromolecules 2020, 53 (7), 2547−2556.

(60) Debuigne, A.; Jérôme, C.; Detrembleur, C. Isoprene-Assisted Radical Coupling of (Co)Polymers Prepared by Cobalt-Mediated Radical Polymerization. Angew. Chem., Int. Ed. 2009, 48 (8), 1422− 1424.

(61) Debuigne, A.; Poli, R.; De Winter, J.; Laurent, P.; Gerbaux, P.; Dubois, P.; Wathelet, J. P.; Jérôme, C.; Detrembleur, C. Cobalt-Mediated Radical Coupling (CMRC): An Unusual Route to Midchain-Functionalized Symmetrical Macromolecules. Chem. - Eur. J. 2010, 16 (6), 1799−1811.

(62) Debuigne, A.; Poli, R.; De Winter, J.; Laurent, P.; Gerbaux, P.; Wathelet, J. P.; Jérôme, C.; Detrembleur, C. Effective Cobalt-Mediated Radical Coupling (CMRC) of Polyvinyl Acetate and Poly(N-Vinylpyrrolidone) (Co)Polymer Precursors. Macromolecules 2010, 43 (6), 2801−2813.

(63) Debuigne, A.; Detrembleur, C.; Jérôme, C.; Junkers, T. Straightforward Synthesis of Symmetrical Multiblock Copolymers by Simultaneous Block Extension and Radical Coupling Reactions. Macromolecules 2013, 46 (22), 8922−8931.

(64) Kermagoret, A.; Chau, N. D. Q.; Grignard, B.; Cordella, D.; Debuigne, A.; Jérôme, C.; Detrembleur, C. Cobalt-Mediated Radical Polymerization of Vinyl Acetate and Acrylonitrile in Supercritical Carbon Dioxide. Macromol. Rapid Commun. 2016, 37 (6), 539−544.

(65) Takeuchi, D.; Iwasawa, T.; Osakada, K. Double-Decker-Type Dipalladium Catalysts for Copolymerization of Ethylene with Acrylic Anhydride. Macromolecules 2018, 51 (14), 5048−5054.

(66) Jian, Z.; Mecking, S. Insertion Homo- and Copolymerization of Diallyl Ether. Angew. Chem., Int. Ed. 2015, 54 (52), 15845−15849.